JOC Article

Conjugated Macrocycles Related to the Porphyrins. 21.† Synthesis, Spectroscopy, Electrochemistry, and Structural Characterization of Carbaporphyrins

Timothy D. Lash,* Michael J. Hayes, John D. Spence,‡ Melanie A. Muckey, Gregory M. Ferrence, and Lisa F. Szczepura

Department of Chemistry, Illinois State University, Normal, Illinois 61790-4160

tdlash@ilstu.edu

Received April 15, 2002

The "3 + 1" variant of the MacDonald condensation has been shown to be an excellent methodology for synthesizing carbaporphyrins. In particular, 1,3-indenedicarbaldehyde condenses with tripyrranes in the presence of TFA to give, following oxidation with DDQ, a series of benzocarbaporphyrins in excellent yields. Triformylcyclopentadienes also afford carbaporphyrin products, albeit in low yields ranging from 5 to 8%. These hybrid bridged annulene structures have porphyrin-like electronic absorption spectra with strong Soret bands near 420 nm and a series of Q-bands through the visible region. The proton NMR spectrum confirms the presence of a strong diamagnetic ring current, and the *meso*-protons show up at 10 ppm, while the internal CH is shielded to approximately −7 ppm. Carbaporphyrins undergo reversible protonation with TFA. Initial addition of acid affords a monocation, although mixtures of protonated species are observed in the presence of moderate concentrations of TFA. However, in the presence of 50% TFA a C-protonated dication is generated. The dications relocate the π-delocalization pathway through the benzo moiety of benzocarbaporphyrins, and these therefore represent bridged benzo[18]annulenes, although they nevertheless retain powerful macrocyclic ring currents. Carbaporphyrins with fused acenaphthylene and phenanthrene rings have been prepared, and the former demonstrated significantly larger bathochromic shifts in UV−vis spectroscopy that parallel previous observations for acenaphthoporphyrins. A diphenyl-substituted benzocarbaporphyrin **19b** was also characterized by X-ray crystallography, and these data show that the macrocycle is reasonably planar although the indene subunit is tilted out of the mean macrocyclic plane by 15.5°. The structural data indicates that the preferred tautomer in the solid state has the two NH's flanking the pyrrolene unit in agreement with previous spectroscopic and theoretical studies. Cyclic voltammetry for carbaporphyrin **19a** was more complex than for true porphyrins, showing five anodic waves and two quasi-reversible reductive couples.

Introduction

The porphyrin macrocycle **1** (Chart 1), which serves as one of Nature's most versatile ligand systems, attracted considerable attention throughout the 20th century.[1] The robust characteristics associated with the porphyrins are due in part to the fully π-delocalized nature of these systems and their associated aromatic character.[2] Aromaticity in porphyrins can be inferred from X-ray crystallography (lack of bond length alternation),[3] calorimetry,[4] and NMR spectroscopy.[5] In particular, porphyrins show powerful diatropic ring currents by proton NMR spectroscopy and this property leads to the external methine or *meso*-protons being shifted downfield to approximately 10 ppm while the internal NHs resonate upfield near −4 ppm.[6] The origin of aromaticity in the porphyrins is often attributed to the presence of an 18π-electron delocalization pathway (indicated in bold)[7] and indeed the porphyrins have been termed the [18]annulenes of Nature.[8] Another view suggests that the "lone pair" electrons of the two pyrrole type nitrogens are also crucial to the aromatic character of porphyrins and that

CHART 1. Carbaporphyrins

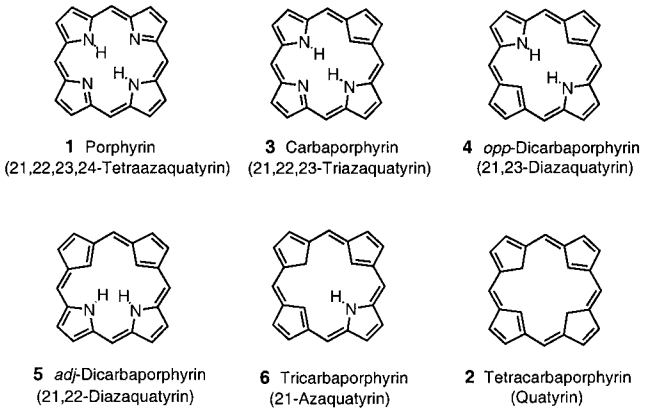

* To whom correspondence should be addressed.

† Part 20: Graham, S. R.; Ferrence, G. M.; Lash, T. D. *Chem. Commun.* **2002**, 894.

‡ Present address: Department of Chemistry, Trinity University, 715 Stadium Drive, San Antonio, TX 78212-7200.

10.1021/jo020267b CCC: $22.00
Published on Web 05/31/2002

the system should be considered a 22π-electron aromatic system.[9] Clearly the nitrogen electrons must have an important influence on the electronic structure of the porphyrins, but it is less obvious how significant the [18]-annulene substructure is in relation to the macrocycle's chemical, physical, and spectroscopic properties. Porphyrin analogues with one or more chalcogen element (O, S, Se, or Te) in place of the usual nitrogen atoms have been known for many years[7,10] but these atoms also provide the equivalent lone pair electrons and so do not allow the two factors to be disentangled. Recently, the possibility of replacing one or more of the nitrogen atoms in the porphyrin macrocycle with carbons has been explored.[8] This approach, in principle, may allow the significance of the 18π-electron core delocalization pathway to be ascertained. The long-term goal of this work is the synthesis of the hypothetical hydrocarbon analogue of the porphyrins **2** which has been named tetracarbaporphyrin or quatyrin (Chart 1).[8] The synthesis of monocarbaporphyrins **3**[11] and an example of an *opp*-dicarbaporphyrin **4**[12] have been previously noted, but the quatyrin system and other intermediary macrocyclic structures such as **5** and **6** are presently unknown (Chart 1).[8] In this paper, the full details of our synthetic studies on monocarbaporphyrins[11,13] and their spectroscopic and electrochemical characterization are reported. In addition, the first structural characterization of a carbaporphyrin by single-crystal X-ray diffraction is described.

Results and Discussion

Monocarbaporphyrins possess an inner core arrangement of three nitrogen atoms and one carbon atom. This CNNN arrangement is also found in the so-called N-confused porphyrins **7** (Chart 2), porphyrin isomers that were originally obtained as byproducts in the Rothemund reaction.[8a,14,15] The incorporation of carbacyclic units into porphyrin-like ring systems required a more directed synthetic approach and a "3 + 1" variant on the MacDonald condensation has been found to be a superior route to systems of this type.[16] The "3 + 1" strategy for porphyrin synthesis involves the condensation of a dialdehyde **8** with a tripyrrolic intermediate **9** known as a tripyrrane (Scheme 1).[16] This methodology has been very effective in the synthesis of porphyrins and has been adapted as a high yielding rational synthesis of alkyl-substituted N-confused porphyrins **10**.[17,18] Porphyrins

(1) (a) Willstatter, R.; Stoll, A. *Untersuchungen uber Chlorophyll*; Springer: Berlin, 1913. (b) Fischer, H.; Orth, H. *Die Chemie des Pyrrols*; Akademische Verlag: Leipzig, 1934; Vol. I. (c) *Ibid*., Vol. II (i), 1937. (d) Fischer, H.; Stern, H., *ibid*., Vol. II (ii), 1940. (e) Lemberg, R.; Legge, J. W. *Haematin Compounds and Bile Pigments*; Interscience: New York, 1949. (f) Vannotti, A. *Porphyrins*; Hilger & Watts, 1954. (g) Falk, H. *Porphyrins and Metalloporphyrins*; Elsevier: Amsterdam, 1964. (h) *The Chlorophylls*; Vernon, L. P.; Seely, G. R., ed.; Academic Press: New York, 1966. (i) Goodwin, T. W. *Porphyrins and Related Compounds*; Academic Press: London, 1968. (j) Marks, G. S. *Heme and Chlorophyll*; Van Nostrand: London, 1969. (k) Jackson, A. H.; Smith, K. M. The Total Synthesis of Pyrrole Pigments. In *The Total Synthesis of Natural Products*; ApSimon, J., Ed.; 1973; Wiley: New York; Vol. 1, pp 143−234. (l) The Chemical and Physical Behavior of Porphyrin Compounds and Related Structures. In *Annals of the New York Academy of Sciences*; Adler, A. D., Ed.; 1973; Vol. 206, pp 1−761. (m) *Porphyrins and Metalloporphyrins*; Smith, K. M., Ed.; Elsevier: Amsterdam, 1975. (n) *The Porphyrins*; Dolphin, D., Ed.; Academic Press: New York, 1978; Vols. 1−7. (o) *Porphyrin Chemistry Advances*; Longo, F. R., Ed.; Ann Arbor Science: Ann Arbor, MI, 1979. (p) Lavallee, D. K. *The Chemistry and Biochemistry of N-Substituted Porphyrins*; VCH: New York, 1987. (q) *Chlorophylls*; Scheer, H., Ed.; CRC Press: Boca Raton, FL. 1991. (r) Milgrom, L. R. *The Colours of Life*; Oxford University Press: New York, 1997. (s) Sessler, J. L.; Weghorn, S. J. *Expanded, Contracted & Isomeric Porphyrins*; Pergamon: Oxford, U.K., 1997. (t) *The Porphyrin Handbook*; Kadish, K. M.; Smith, K. M.; Guilard, R., Eds.; Academic Press: San Diego, 2000; Vols. 1−10.

(2) Vogel, E. *J. Heterocycl. Chem*. **1996**, *33*, 1461.

(3) Senge, M. O. In *The Porphyrin Handbook*; Kadish, K. M.; Smith, K. M.; Guilard, R., Eds.; Academic Press: San Diego, 2000; Volume 10.

(4) Stern, A.; Klebs, G. *Ann. Chem*. **1932**, *500*, 91; **1933**, *504*, 287; **1933**, *505*, 295.

(5) Janson, T. R.; Katz, J. J. In *The Porphyrins*; Dolphin, D., Ed.; Academic Press: New York, 1978; Vol. 4, pp 1−59. Scheer, H.; Katz, J. J. In *Porphyrins and Metalloporphyrins*; Smith, K. M., Ed.; Elsevier: Amsterdam, 1975; pp 399−524. Medforth, C. J. In *The Porphyrin Handbook*; Kadish, K. M.; Smith, K. M.; Guilard, R., Eds.; Academic Press: San Diego, 2000; Vol. 5, pp 1−80. Chakraborty, S.; Clezy, P. S.; Sternhell, S.; van Thuc, L. *Aust. J. Chem*. **1982**, *35*, 2315. Crossley, M. J.; Harding, M. M.; Sternhell, S. *J. Am. Chem. Soc*. **1992**, *114*, 3266.

(6) Smith, K. M. in *Porphyrins and Metalloporphyrins*; Smith, K. M., Ed.; Elsevier: New York, 1975; pp 3−28.

(7) Vogel, E.; Haas, W.; Knipp, B.; Lex, J.; Schmickler, H. *Angew. Chem., Int. Ed. Engl*. **1988**, *27*, 406.

(8) (a) Lash, T. D. *Synlett* **2000**, 279. (b) Lash, T. D. In *The Porphyrin Handbook*; Kadish, K. M.; Smith, K. M.; Guilard, R., Eds.; Academic Press: San Diego, 2000; Vol. 2, pp 125−199.

(9) Cyranski, M. K.; Krygowski, T. M.; Wisiorowski, M.; Hommes, N. J. R. van E.; Schleyer, P. von R. *Angew. Chem., Int. Ed*. **1998**, *37*, 177.

(10) Johnson, A. W. in *Porphyrins and Metalloporphyrins*; Smith, K. M., Ed.; Elsevier: Amsterdam, 1975; pp 729−754. Latos-Grazynski, L. In *The Porphyrin Handbook*; Kadish, K. M.; Smith, K. M.; Guilard, R., Eds.; Academic Press: San Diego, 2000; Vol. 2, pp 361−416. Broadhurst, M. J.; Grigg, R.; Johnson, A. W. *J. Chem. Soc. (C)* **1971**, 3681. Ulman, A.; Manassen, J. *J. Am. Chem. Soc*. **1975**, *97*, 6540. *Ibid., J. Chem. Soc., Perkin Trans. 1* **1979**, 1066. Lash, T. D.; Motta, Y. G. *Heterocycles* **1983**, *20*, 2343. Haas, W.; Knipp, B.; Sicken, M.; Lex, J.; Vogel, E. *Angew. Chem., Int. Ed. Engl*. **1988**, *27*, 409. Vogel, E.; Rohrig, P.; Sicken, M.; Knipp, B.; Herrmann, A.; Pohl, M.; Schmickler, H.; Lex, J. *Angew. Chem., Int. Ed. Engl*. **1989**, *28*, 1651. Lash, T. D.; Armiger, Y. L. S.-T. *J. Heterocycl. Chem*. **1991**, *28*, 965. Vogel, E.; Pohl, M.; Herrmann, A.; Wiss, T.; König, C.; Lex, J.; Gross, M.; Gisselbrecht, J. P. *Angew. Chem., Int. Ed. Engl*. **1996**, *35*, 1520. Chmielewski, P. J.; Latos-Grazynski, L.; Olmstead, M. M.; Balch, A. L. *Chem. Eur. J*. **1997**, *3*, 268. Gross, Z.; Saltsman, I.; Pandian, R. P.; Barzilay, C. M. *Tetrahedron Lett*. **1997**, *38*, 2383.

(11) Preliminary communication: Lash, T. D.; Hayes, M. J. *Angew. Chem., Int. Ed. Engl*. **1997**, *36*, 840.

(12) Lash, T. D.; Romanic, J. L.; Hayes, M. J.; Spence, J. D. *Chem. Commun*. **1999**, 819.

(13) These results were presented, in part, at the following meetings and symposia: Symposium on Advances in Natural Products Synthesis, 28th Central Regional Meeting of the American Chemical Society, Dayton, OH, June 1996 (Lash, T. D. *Program and Abstracts*, Abstract No. 201); 89th Annual Meeting of the Illinois State Academy of Science, Illinois Wesleyan University, Bloomington, IL, October 1996 (Hayes, M. J.; Lash, T. D. Transactions of the Illinois State Academy of Science, 1996, Supplement to Volume 89, p 55, Abstract No. 46); 213th National Meeting of the American Chemical Society, San Francisco, CA, April 1997 (Lash, T. D. *Book of Abstracts*, ORGN 14 and Hayes, M. J.; Lash, T. D. *Book of Abstracts*, ORGN 297); 30th Great Lakes Regional Meeting of the American Chemical Society, Loyola University, Chicago IL, May 1997 (Hayes, M. J.; Lash, T. D. *Program and Abstracts*, Abstract No. 128; Lash, T. D. *Program and Abstracts*, Abstract No. 142); 5th Chemical Congress of North America, Cancun, Mexico, November 1997 (Lash, T. D.; Chaney, S. T.; Hayes, M. J.; Petryka, J. C.; Richter, D. T. *Book of Abstracts*, Abstract No. 1154); 221st National Meeting of the American Chemical Society, San Diego, CA, April 2001 (Muckey, M. A.; Lash, T. D. *Book of Abstracts*, ORGN 715). A popularized account of these studies and related work also appeared: Freemantle, M. Porphyrin Route Revival: Aromatic Porphyrinoids Synthesized by '3 + 1' Condensation. *Chem. Eng. News* **1997**, *75* (35), 31−33.

(14) (a) Chmielewski, P. J.; Latos-Grazynski, L.; Rachlewicz, K.; Glowiak, T. *Angew. Chem. Int. Ed. Eng*. **1994**, *33*, 779. (b) Furuta, H.; Asano, T.; Ogawa, T. *J. Am. Chem. Soc*. **1994**, *116*, 767.

(15) Geier, G. R., III; Haynes, D. M.; Lindsey, J. S. *Org. Lett*. **1999**, *1*, 1455. Geier, G. R., III; Ciringh, Y.; Li, F.; Haynes, D. M.; Lindsey, J. S. *Org. Lett*. **2000**, *2*, 1745.

(16) Lash, T. D. *Chem. Eur. J*. **1996**, *2*, 1197. Lin, Y.; Lash, T. D. *Tetrahedron Lett*. **1995**, *36*, 9441. Lash, T. D. *J. Porphyrins Phthalocyanines* **1997**, *1*, 29.

CHART 2. Carbaporphyrinoids and Related Macrocyclic Systems

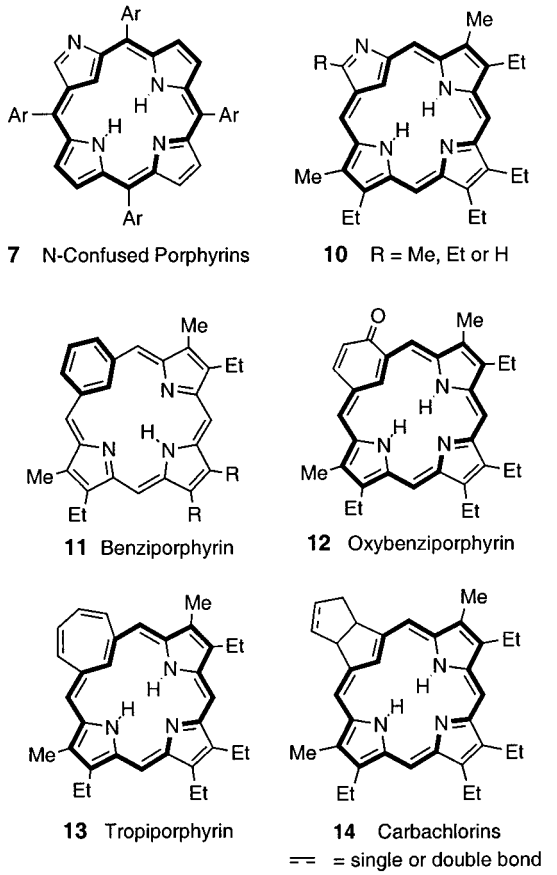

SCHEME 1

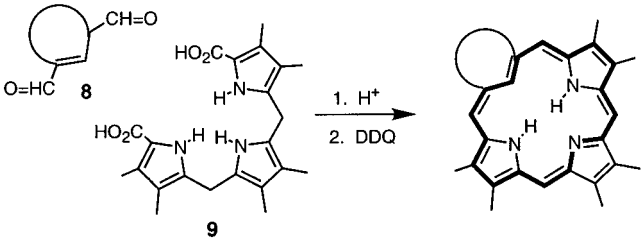

with carbacyclic rings are easily prepared by this approach: for instance, isophthalaldehyde affords benziporphyrin **11**,[19,20] 5-formylsalicylaldehyde gives oxybenziporphyrin **12**,[20−22] 1,6-diformyl-1,3,5-cycloheptatriene yields tropiporphyrin **13**,[23] and bicyclo[3.3.0]octane dialdehydes produced carbachlorins **14**[24] (Chart 2). Complex mixtures of true carbaporphyrins **15** were first obtained by the "3 + 1" condensation of 1,3-azulenedicarbaldehyde (**16**) with tripyrrane **17** in the presence of HBr, followed

SCHEME 2

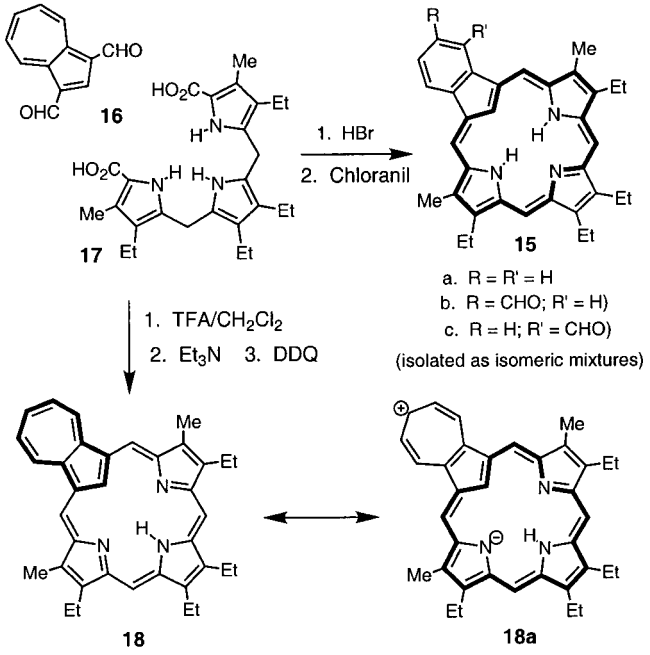

by oxidation with chloranil (Scheme 2).[25] In surprising contrast, Lash and Chaney found that **16** and **17** condensed in the presence of TFA in dichloromethane to give, following oxidation with DDQ, the cross-conjugated porphyrinoid macrocycle azuliporphyrin (**18**) in 28% yield.[26] This system was quite stable and showed a degree of aromatic character due to zwitterionic canonical forms such as **18a**.[26] Subsequently, Lash demonstrated that azuliporphyrin rearranged under basic oxidative conditions with *tert*-butyl hydroperoxide to give benzocarbaporphyrins **15** and a mechanism to explain this unusual rearrangement was proposed.[27] In independent work, we developed a rational synthesis of benzocarbaporphyrins **19** using indene dialdehyde **20** as the key precursor (Scheme 3).[11] Tripyrrane dibenzyl esters **21** are easily prepared by condensing 2,5-unsubstituted pyrroles **22** with 2 equiv of an acetoxymethylpyrrole **23** in the presence of an acid catalyst.[16,28] Hydrogenolysis of the benzyl esters over 10% Pd/C affords the corresponding relatively unstable dicarboxylic acids **24** in quantitative yields.[16,28] Treatment of tripyrranes **24** with TFA, followed by dilution with dichloromethane, reaction with **20** under N_2 and subsequent neutralization with triethylamine and dehydrogenation with DDQ affords the benzocarbaporphyrins **19** in 43−51% yield. Most of our early studies were carried out on tetraethylcarbaporphyrin **19a**[11,29] and the discussion on the properties of carbaporphyrins will mostly focus on this compound. However, unless otherwise noted, the spectroscopic properties of the other monocarbaporphyrins presented in this paper were similar to those for **19a**.

(17) Lash, T. D.; Richter, D. T.; Shiner, C. M. *J. Org. Chem.* **1999**, *64*, 7973.
(18) For a "2 + 2" MacDonald synthesis of N-confused porphyrins, see: Liu, B. Y.; Brückner, C.; Dolphin, D. *Chem. Commun.* **1996**, 2141.
(19) Berlin, K.; Breitmaier, E. *Angew. Chem., Int. Ed. Engl.* **1994**, *33*, 1246.
(20) Lash, T.D.; Chaney, S. T.; Richter, D. T. *J. Org. Chem.* **1998**, *63*, 9076.
(21) Lash, T. D. *Angew. Chem., Int. Ed. Engl.* **1995**, *34*, 2533. See also: Lash, T. D.; Chaney, S. T. *Chem. Eur. J.* **1996**, *2*, 944
(22) Richter, D. T.; Lash, T. D. *Tetrahedron* **2001**, *57*, 3659.
(23) Lash, T. D.; Chaney, S. T. *Tetrahedron Lett.* **1996**, *37*, 8825.
(24) Hayes, M. J.; Lash, T. D. *Chem. Eur. J.* **1998**, *4*, 508.
(25) (a) Berlin, K.; Steinbeck, C.; Breitmaier, E. *Synthesis* **1996**, 336. (b) Berlin, K. *Angew. Chem. Int. Ed. Engl.* **1996**, *35*, 1820.
(26) Lash, T. D.; Chaney, S. T. *Angew. Chem., Int. Ed. Engl.* **1997**, *36*, 839. Graham, S. R.; Colby, D. A.; Lash, T. D. *Angew. Chem., Int. Ed.* **2002**, *41*, 1371.
(27) Lash, T. D. *Chem. Commun.* **1998**, 1683.
(28) Sessler, J. L.; Johnson, M. R.; Lynch, V. *J. Org. Chem.* **1987**, *52*, 4394.
(29) Hayes, M. J.; Spence, J. D.; Lash, T. D. *Chem. Commun.* **1998**, 2409.

SCHEME 3

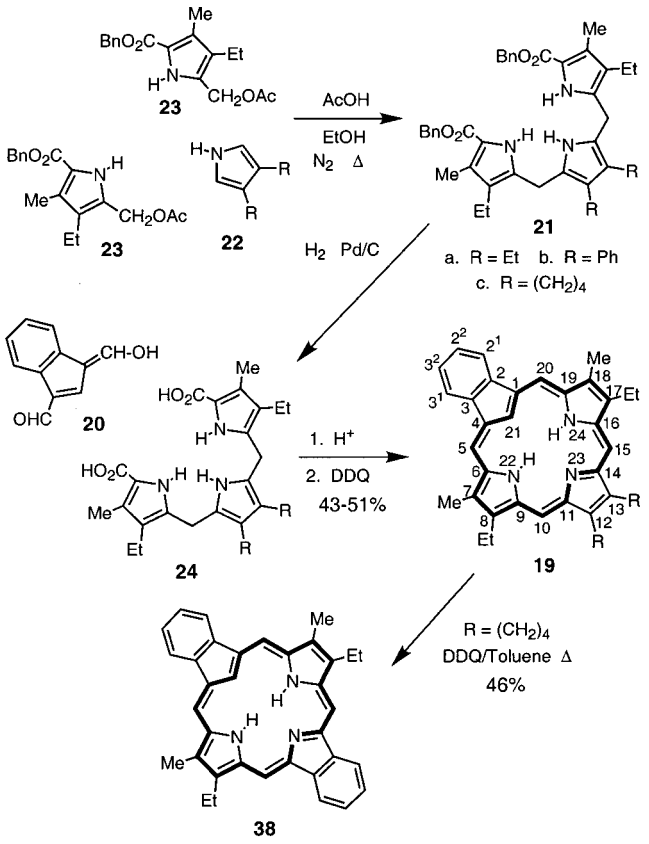

Porphyrins have characteristic UV−vis absorption spectra that show a strong Soret band near 400 nm followed by a series of four Q-bands through the visible region. If carbaporphyrins retain porphyrin-like properties, one would expect that they would also have the same type of electronic absorption spectra. This is evidently the case, as **19a** shows a Soret band at 424 nm (log ϵ = 5.25) and four Q-bands at 510, 544, 602, and 662 nm (Figure 1A). These bands have undergone small bathochromic shifts compared to the related benzoporphyrin **25** (Chart 3) which shows the Soret absorption at 404 nm (log ϵ = 5.46) and Q-bands at 504, 542, 574, and 628 nm (Figure 2A).[30] The Soret band of **19a** is less intense, and a secondary band is also evident at 376 nm. Diphenylcarbaporphyrin **19b** gave slightly red-shifted absorptions compared to **19a**, and the Soret band was somewhat intensified. On the other hand, butanocarbaporphyrin **19c** gave a virtually identical spectrum to **19a**.

Addition of TFA to solutions of **19a** leads to protonation, but mixtures of species appear to be present and the results are of little diagnostic value at moderate concentrations of TFA. However, in 50% TFA−$CHCl_3$ a deep green colored diprotonated species **26** was generated, and this showed a moderate band at 348 nm, a Soret absorption at 426 nm (log ϵ = 5.27) and weaker absorptions at 614 and 662 nm (Figure 1B). Not surprisingly, the UV−vis spectrum for the diprotonated form of benzoporphyrin **25** in 5% TFA−$CHCl_3$ is quite different, showing a far stronger Soret band at 414 nm, and weaker absorptions at 562 and 612 nm (Figure 2B). At very low concentrations of TFA (0.005−0.1% TFA−CH_2Cl_2), benzocarbaporphyrin **19a** gave rise to another green colored species that showed multiple peaks in the Soret band region. This was attributed to the monocation **27** (Scheme 4).

Proton NMR spectroscopy provided strong support for the porphyrin-like nature of carbaporphyrins **19**. The powerful diatropic ring current in **19a** is evident in the proton NMR spectrum (Figure 3) as the bridging methine or *meso*-protons were shifted downfield to 9.8 and 10.1 ppm, while the internal CH shifted upfield to near −7 ppm (this value varied slightly with concentration). The NHs were also strongly shielded and gave a broad resonance near −4 ppm. As is the case for porphyrins, the alkyl substituents were also strongly effected by the aromatic ring current with the methyl groups showing up at 3.6 ppm while the ethyl methylenes resonated near 4 ppm. The protons on the benzo moiety adjacent to the porphyrinoid macrocycle were also strongly influenced and resonated near 8.8 ppm. In independent work by Breitmaier and co-workers, low yields of carbaporphyrins were obtained using related chemistry.[25] In these samples, the presence of tautomers (e.g., **28**, Scheme 5) that did not interconvert on the NMR time scale were postulated on the basis of additional peaks that were present in the proton NMR spectra.[25] We deacidify the $CDCl_3$ for our studies by running the solvent through a small amount of basic alumina. If the solvent is not pretreated, additional peaks may show up due to the presence of protonated species. However, using deacidified $CDCl_3$ we have never seen any of the extra peaks that were noted by this group. While it is possible that the extra peaks observed by Breitmaier and co-workers[25] may have arisen due to spurious protonation, we have suggested previously that they are most likely due to isomeric impurities.[11,20] Under certain acid-catalyzed conditions, the tripyrrane intermediates may undergo acidolysis and subsequent recombination of the resulting fragments can lead to isomeric tripyrroles which in turn would give rise to mixtures of macrocyclic products. A more detailed discussion on this issue has been published elsewhere,[20] and in the absence of evidence to the contrary it is assumed that this is the correct interpretation of the available data.

Although two similar tautomers can be considered for **19a** (Scheme 5), theoretical studies suggest that tautomer **19a** with two NHs flanking the imine nitrogen is favored over **28a** by 6 kcal/mol.[33] This is primarily due to the presence of more favorable hydrogen bonding interactions as the three inner hydrogens have similar steric interactions in both forms. Our NMR data is consistent with the presence of either a single tautomer **19a** with a plane of symmetry, or with the presence of mixed tautomers that rapidly interconvert on the NMR time scale. In variable temperature studies, little change was observed between the room-temperature spectrum and the spectra at −50 or −75 °C apart from a sharpening up of the NH resonance (Figure 3). The CH proton does shift slightly

(30) Hayes, M. J. M. S. Thesis, Illinois State University, 1997.

(31) Lash, T. D. *Energy Fuels* **1993**, *7*, 166.

(32) (a) Clezy, P. S.; Fookes, C. J. R.; Mirza, A. H. *Aust. J. Chem.* **1977**, *30*, 1337. (b) Clezy, P. S.; Mirza, A. H. *Aust. J. Chem.* **1982**, *35*, 197. (c) Clezy, P. S.; Leung, C. W. F. *Aust. J. Chem.* **1993**, *46*, 1705.

(33) Ghosh, A.; Wondimagegn, T.; Nilsen, H. J. *J. Phys. Chem. B* **1998**, *102*, 10459. See also: Nilsen, H. J.; Ghosh, A. *Acta Chem. Scand.* **1998**, *52*, 827. Ghosh, A. *Angew. Chem. Int. Ed. Engl.* **1995**, *34*, 1028. Ghosh, A. *Acc. Chem. Res.* **1998**, *31*, 189.

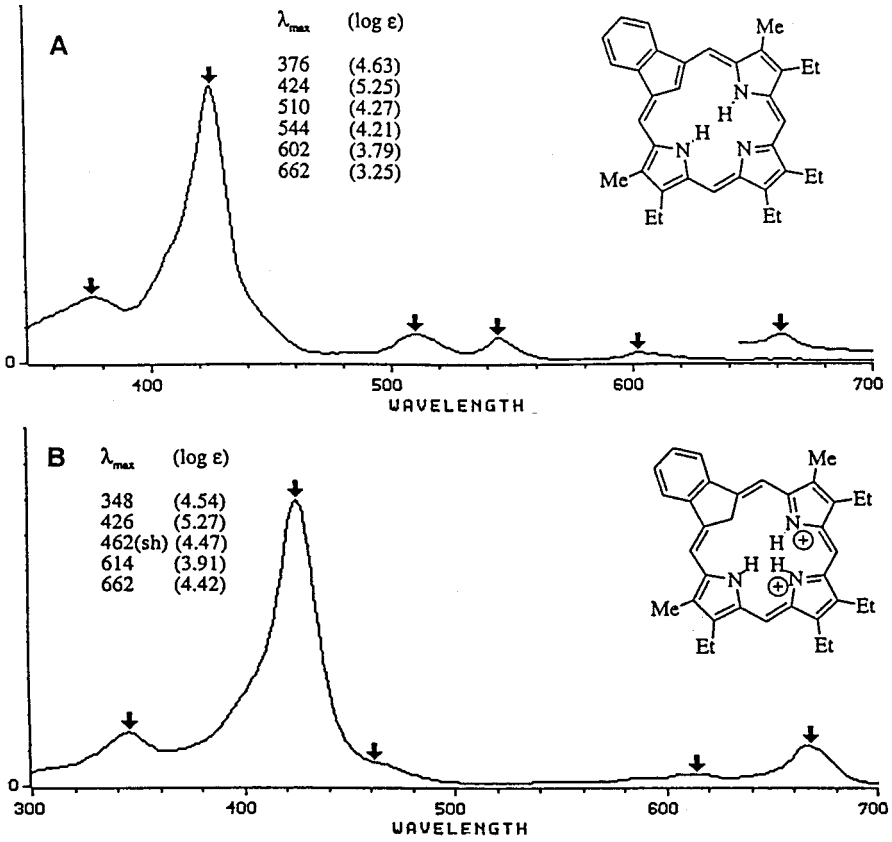

FIGURE 1. UV−vis spectra of benzocarbaporphyrin **19a**. A. Free base in 1% triethylamine−chloroform. B. Dication **26** in 50% TFA−chloroform.

CHART 3

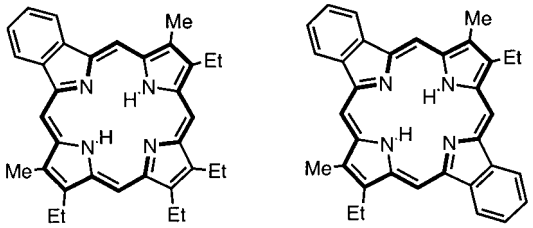

25 **39**

upfield, but this is also observed at higher concentrations and is most likely due to aggregation effects. While these data do not distinguish between a preference for a single tautomer vs rapid exchange, it nonetheless limits the possibilities. Carbon-13 NMR spectroscopy also confirms that **19a** has a plane of symmetry with 5 sp^3 carbon resonances between 11.7 and 20.3 ppm, two *meso*-carbons appearing at 95.1 and 100.2 ppm (these values are similar to those observed for true porphyrins), and the 11 other types of sp^2 carbons expected based on symmetry considerations produced 10 resonances between 109 and 146 ppm. The internal CH is present at 109.7 ppm. Again no evidence for the presence of tautomers was found in any of the carbon-13 spectra that were run on these compounds. The structures of carbaporphyrins **19** were further confirmed by mass spectrometry.

Recently, Furuta has demonstrated that *meso*-tetraphenyl N-confused porphyrin exists as the aromatic tautomer **7** in $CDCl_3$, but prefers a cross-conjugated tautomer with an external NH in DMF solution.[34] Density functional theory indicates that these two forms only differ in stability by 5.7 kcal/mol.[33,35] We took the opportunity to examine the previously synthesized heptaalkyl N-confused porphyrin **10a**.[17] Interestingly, the proton NMR spectrum for **10a** in d_7-DMF at 21 °C showed the presence of two tautomeric forms in an approximately 1:1 ratio (Figure 4A). The aromatic form **10a** was evident from the four downfield singlets between 9.8 and 10.2 ppm corresponding to the *meso*-protons and the upfield resonances at −6.29, −3.61, and −3.71 ppm due to the internal CH and two nonequivalent NH protons. The cross-conjugated tautomer **29** (Chart 4) gave three singlets for the *meso*-protons at 8.53, 8.80, and 9.12 ppm in the ratio of 2:1:1 and a broad singlet at 13.57 ppm for the external NH. The inner CH resonated at −0.07 ppm, a value that is comparable to the resonance observed by Furuta for the corresponding CH in **7** at +0.76 ppm.[34] Tautomer **29** is clearly stabilized by dipolar contributors such as **30** that provide a degree of aromatic character to the system.[36] The balance is further influenced by favorable hydrogen bonding between the DMF and the external NH of **29**. It is noteworthy that the rate of interconversion between **10** and **29** must be relatively slow. In addition, the two inner NHs of the aromatic form

(34) Furuta, H.; Ishizuka, T.; Osuka, A.; Dejima, H.; Nakagawa, H.; Ishikawa, I. *J. Am. Chem. Soc.* **2001**, *123*, 6207.

(35) Ghosh, A. In *The Porphyrin Handbook*; Kadish, K. M.; Smith, K. M.; Guilard, R., Eds.; Academic Press: San Diego, 2000; Vol. 7, pp 1−38.

(36) In this respect, the system resembles azuliporphyrin **18**.[26]

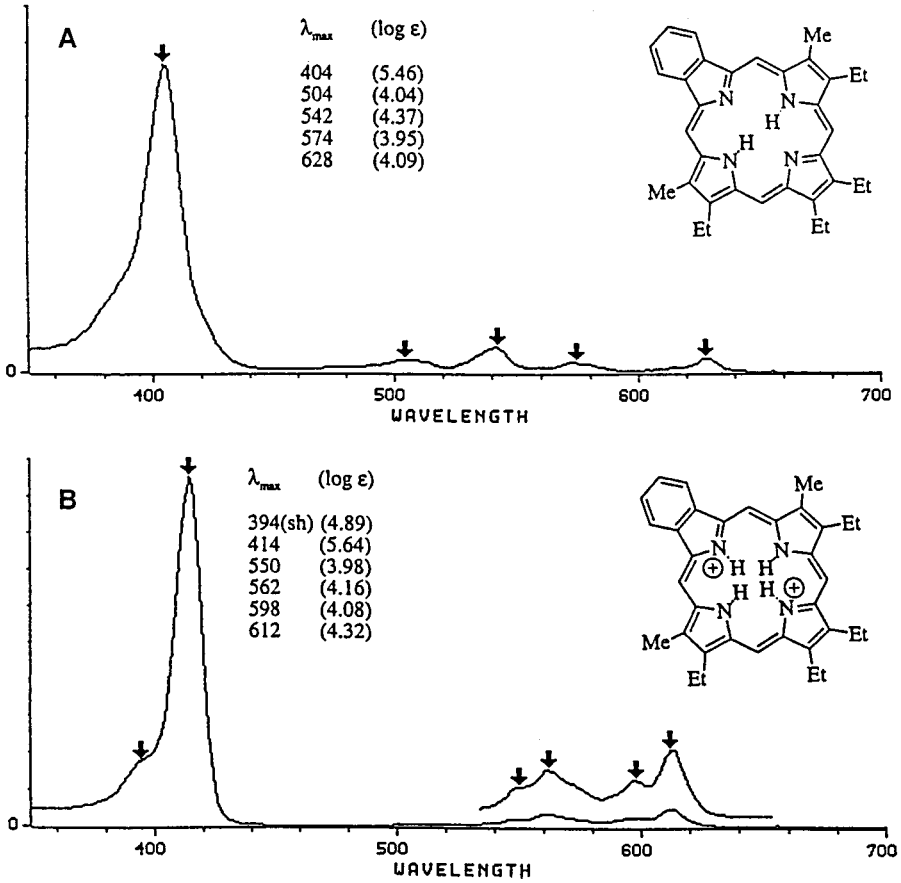

FIGURE 2. UV−vis spectra of benzoporphyrin **25**. A. Free base in 1% triethylamine−chloroform. B. Dication in 5% TFA−chloroform.

SCHEME 4

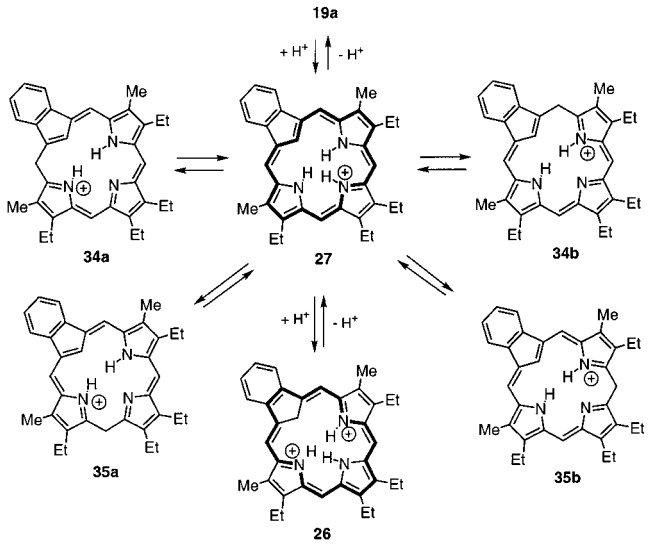

10 are well resolved at 21 °C, indicating that only one aromatic tautomer is favored and that the NH exchange rate within the macrocyclic cavity is also slow on the NMR time scale. At 50 °C, the spectrum was little effected, and no indication of coalescence for any of these processes was observed. The proton NMR spectrum of benzocarbaporphyrin **19a** in d_7-DMF, on the other hand, gave much the same results as in $CDCl_3$, although the NH resonance was relatively sharp and there is a slight downfield shift for the *meso*- and benzo-protons (Figure 4B).

Addition of trace amounts of TFA to NMR solutions of **19a** in $CDCl_3$ afforded the monocation **27** where the first protonation has occurred as expected at the pyrrolene nitrogen (Scheme 4). The proton NMR spectrum for **27** showed the inner CH at −6.75 ppm, while the NHs gave two broadened singlets at −4.61 (1H) and −3.22 ppm (2H). The plane of symmetry for the macrocycle in the monocation was retained as judged by the simplicity of the proton NMR spectrum, and the *meso*-protons gave rise to two 2H singlets at 10.06 and 10.33 ppm. Addition of further amounts of TFA produced complex proton NMR spectra showing the presence of mixtures of different species. However, in 50% TFA−$CDCl_3$ a single species was observed that could be assigned as the C-protonated dication **26** (Scheme 4). The proton NMR spectrum shows that **26**, like **27**, retains a strong diamagnetic ring current (Figure 5). The *meso*-protons resonated at 10.45 and 11.05 ppm while the internal CH_2 was shifted upfield to −5.14 ppm, and the NH protons were observed at −1.4 ppm. The benzo-protons adjacent to the macrocyclic ring were shifted downfield to 10.13 ppm compared to 8.83 ppm in the free base and 8.69 for the monocation, while the remaining benzo-protons resonated at 8.94 ppm compared to 7.74 for **19a** and 7.72 ppm for **27**. These shifts cannot be simply due to the dicationic nature of this species and are instead consistent with the 18π-electron delocalization pathway having been relocated

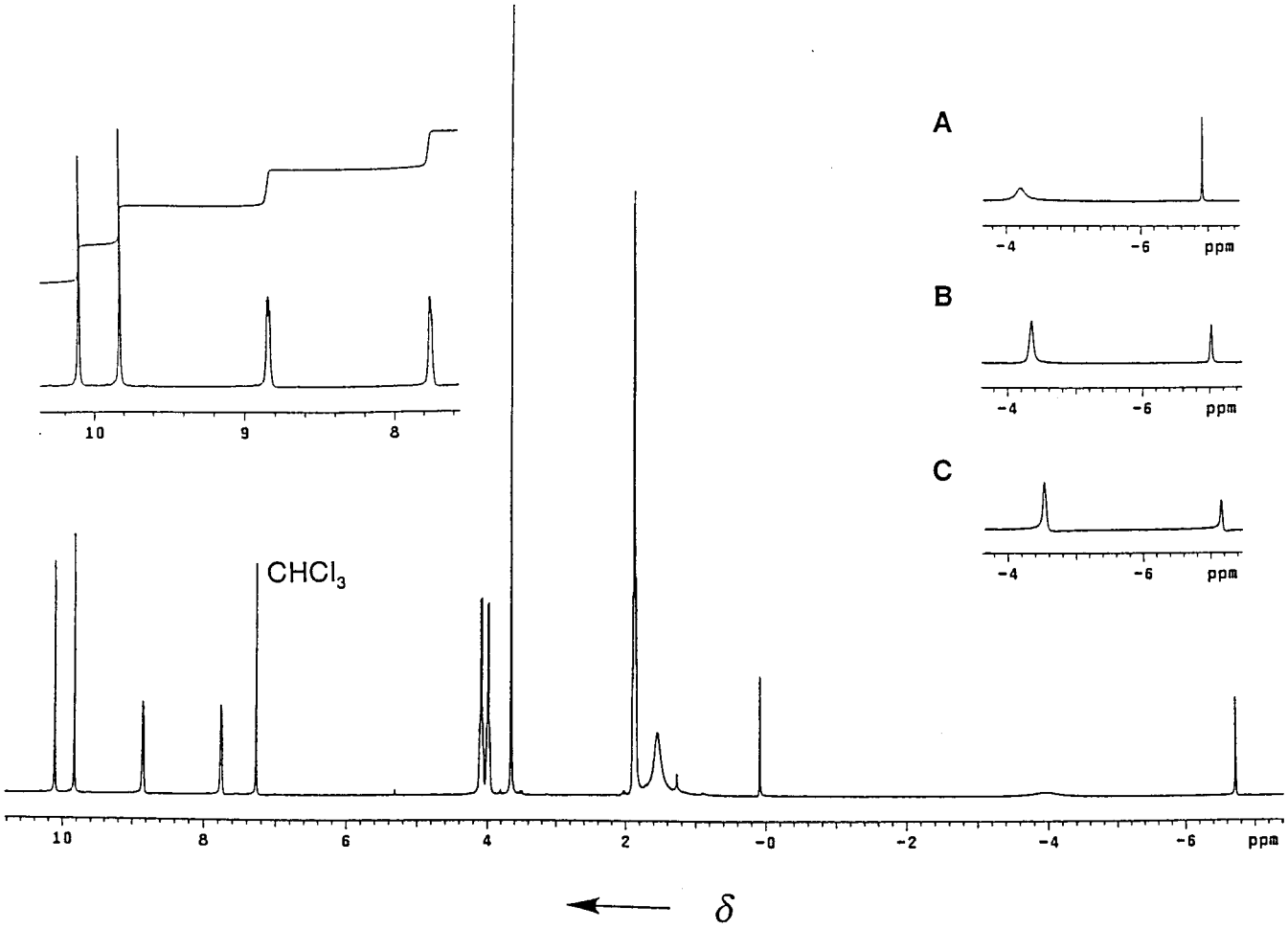

FIGURE 3. 400 MHz proton NMR spectrum of benzocarbaporphyrin **19a** in deuteriochloroform at 25 °C. A. Upfield region at −25 °C; B. −50 °C; C. −75 °C. At low temperatures some peak broadening occurs due to precipitation of the sample.

SCHEME 5

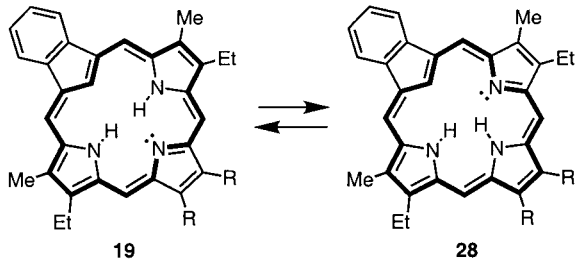

through the benzene ring (see bold pathway for structure **26**). The dication is, therefore, an example of a bridged benzo[18]annulene. Benzo[18]annulene **31** (Chart 5) has a weakly diatropic nature, and the difference in chemical shifts ($\Delta\delta$) between the inner and outer macrocyclic ring protons is only 3.3 ppm.[37] In complete contrast, the $\Delta\delta$ for the internal vs external CH resonances of **26** are on the order of 16 ppm! Therefore, the characteristics of **26** are quite different from the parent system, and this can be attributed to the enhanced charged delocalization that is only possible in the fully delocalized aromatic structure. Dicarbaporphyrin **32** has been shown to undergo C-protonation in the presence of trace amounts of TFA to give the fully aromatic benzo[18]annulene monocation **33** (Chart 5).[12] In this case, C-protonation occurs more easily as this results in only one delocalized positive charge.[12,38] At room temperature the NH protons produced a broad peak that only integrated for 2H, but at −10 °C the 2H resonance sharpened up and an additional broad signal for 1H can be discerned. These data indicates that one proton for the internal NH's undergoes intermolecular exchange while the other two are held more firmly. A similar phenomenon was also observed for the dication of N-confused porphyrin **10a**.[17] Addition of 50% *d*-TFA to NMR solutions of **19a** in $CDCl_3$ resulted in a slow deuterium exchange of the *meso*-protons (approximately 20−30% loss of signal intensity after 16 h at room temperature). Similar exchange rates at the *meso*-positions were noted in the presence of trace *d*-TFA, and these data suggest that the monocation **27** is in equilibrium with C-protonated species such as **34** and **35** (Scheme 4). It is possible that similar diprotonated species are also present in these equilibria. However, under both sets of conditions, exchange at the C-10 and C-15 positions occurred approximately 50% faster than at the C-5 and C-20 positions. As would be expected, rapid exchange of the NH and inner CH protons is also

(37) Meissner, U. E.; Gensler, A.; Staab, H. A. *Tetrahedron Lett.* **1977**, *18*, 3.

(38) C-protonation is also observed for carbasapphyrins: Lash, T. D.; Richter, D. T. *J. Am. Chem. Soc.* **1998**, *120*, 9965.

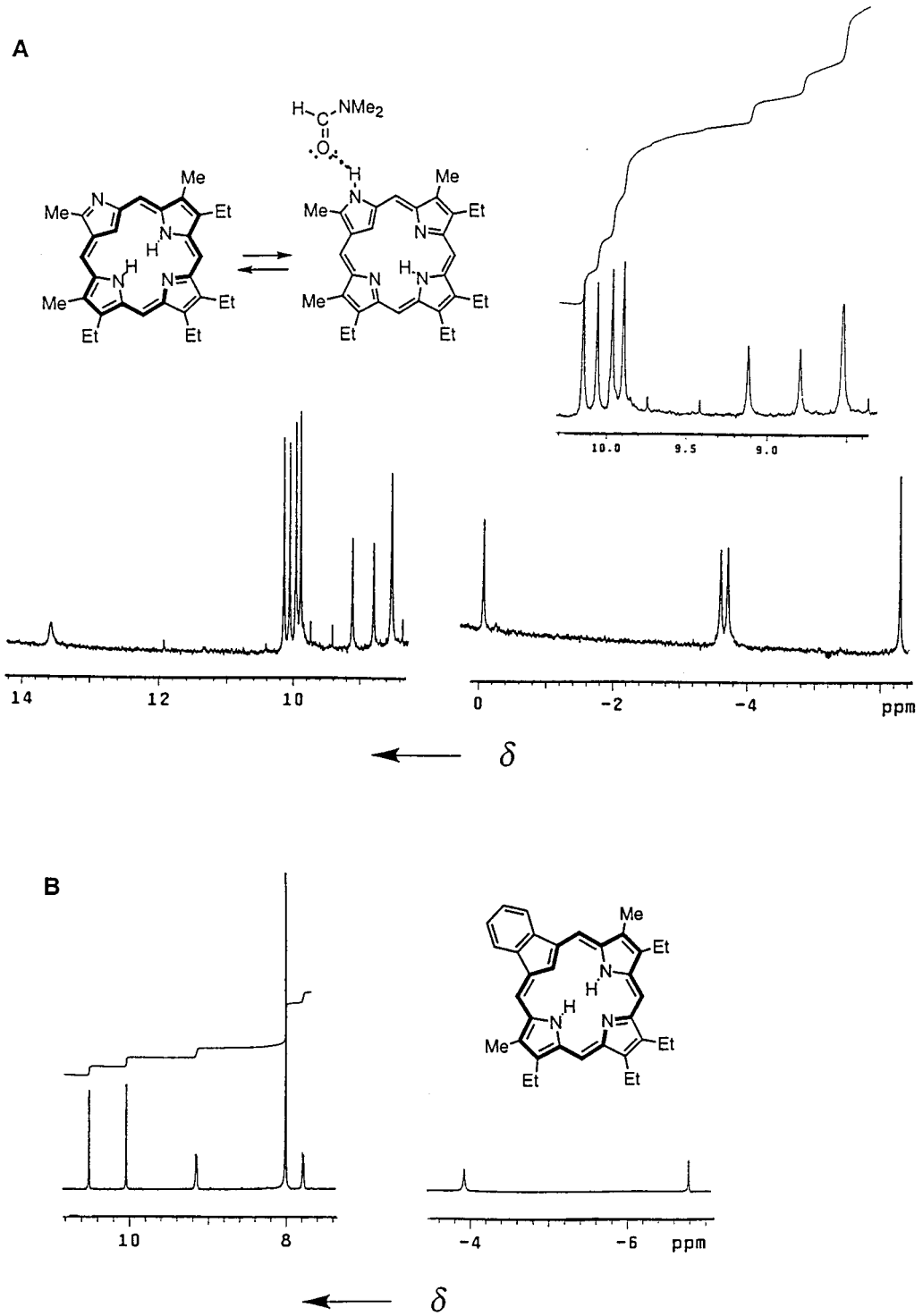

FIGURE 4. (A) Upfield and downfield regions of the 400 MHz proton NMR spectrum for N-confused porphyrin **10a** in d_7-DMF. The presence of two tautomers, **10a** and **29**, are evident. The sample shows signs of significant degradation on standing in this solvent. (B) Upfield and downfield regions of the 400 MHz proton NMR spectrum for benzocarbaporphyrin **19a** in d_7-DMF.

observed in these experiments. The carbon-13 NMR spectrum of **26** in 50% TFA−$CDCl_3$ shows the presence of a plane of symmetry with five sp^3 carbon resonances between 11 and 21 ppm, the internal CH_2 at 32.9 ppm, and two *meso*-carbons near 108 ppm; nine additional sp^2 signals were observed for the 10 remaining carbons between 125 and 152 ppm.

In other work, we have examined the effects of fusing aromatic rings onto the porphyrin nucleus.[31,39−43] Specifically, the introduction of fused benzene (e.g., **25**)[31,32] or phenanthrene rings (e.g., **36**, Chart 6)[40] onto the porphyrin chromophore resulted in only small bathochromic

(39) Lash, T. D. *J. Porphyrins Phthalocyanines* **2001**, *5*, 267.
(40) Lash, T. D.; Novak, B. H. *Ang. Chem. Int. Ed. Engl.* **1995**, *34*, 683. Novak, B. H.; Lash, T. D. *J. Org. Chem.* **1998**, *63*, 3998.
(41) Lash, T. D.; Chandrasekar, P.; Osuma, A. T.; Chaney, S. T.; Spence, J. D. *J. Org. Chem.* **1998**, *63*, 8455.
(42) Lash, T. D.; Chandrasekar, P. *J. Am. Chem. Soc.* **1996**, *118*, 8767. Spence, J. D.; Lash, T. D. *J. Org. Chem.* **2000**, *65*, 1530−1539.

CHART 4

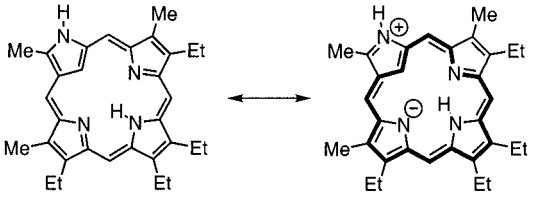

shifts in UV−vis spectroscopy, but acenaphthylene-fused porphyrins (e.g., **37**, Chart 6) gave rise to greatly altered UV−vis spectra that showed much larger shifts toward longer wavelengths.[41,42] It was therefore of some interest to see whether these trends also held for the carbaporphyrin series. Dibenzocarbaporphyrin **38** was easily prepared by dehydrogenating the butano derivative **19c** with 2 equiv of DDQ in refluxing toluene (Scheme 3).[31] The addition of a second fused benzene ring causes the Soret band for **38** to shift to 432 nm from 424 nm for **19a**. This contrasts to dibenzoporphyrin **39**[30,44] which shows a Soret band at 410 nm compared to a value of 404 nm in the case of monobenzoporphyrin **25** (Chart 3). Reaction of the known acenaphthotripyrranes **40**[41] with diformylindene **20** under standard "3 + 1" conditions gave the corresponding acenaphthocarbaporphyrins **41** in 18−29% yield, while phenanthrotripyrrane **42** gave the corresponding phenanthrocarbaporphyrin **43** in 28% yield (Scheme 6). The spectroscopic properties of **38**, **41**, and **43** are fully consistent with the assigned structures. Dibenzocarbaporphyrin **38** shows a Soret band at 432 nm, while the value for **43** is 442 nm and for acenaphthocarbaporphyrin **41a** the absorption appears at 456 nm. The longest wavelength Q-band absorptions for **19a**, **38**, **43**, and **41a** are 662, 672, 677, and 688 nm (this band is very weak for **41a**), respectively, again showing the largest effects for the acenaphthylene-fused porphyrinoids. The trend is more gradual in the carbaporphyrin series than has been observed for true porphyrins,[39] although it is comparable to the results for oxybenzi- and oxypyriporphyrins.[20] The same trends are observed for the corresponding dications in 50% TFA−chloroform and the Soret band for **41a** under these conditions shifts to 474 nm.

Triformylcyclopentadienes **44** have also been reported to react with tripyrrane **24a** to give low yields of carbaporphyrins (Scheme 7).[25b] In the initial publication, these porphyrinoids also showed additional peaks that were attributed to tautomers. We have synthesized formylcarbaporphyrins **45a** and **45b** under our reaction conditions and find no sign of the extra resonances in any of the NMR spectra. In addition, the UV−vis absorptions for our samples gave molar extinction coefficients for the major absorptions that were nearly 3 times larger than those in the earlier report. The UV−vis spectrum of **45a** is substantially different from benzocarbaporphyrin **19a**, showing a weaker broadened Soret band at 436 nm, but this nonetheless retains the essential features of a porphyrin-type electronic spectrum (Figure 6). At low concentrations of TFA (0.01%), a new species is observed that shows a series of moderate absorptions through the Soret band region; this species was assigned as the monocation **46**. In 40% TFA−chloroform, the corresponding dication **47** was generated. This shows a split Soret band at 410 and 426 nm and three smaller absorptions at 548, 600, and 664 nm. The yields for porphyrinoids **44** were low, generally 5−8%, most likely due to the unwanted reactivity of the third formyl moiety. Attempts to improve these yields were not successful. We have found that in some reactions substituting a wash with dilute aqueous ferric chloride solution for the oxidation step with DDQ can give much improved yields,[17,45] but this procedure gave essentially the same results in the present case.

The proton NMR spectra for **45a** and **45b** in $CDCl_3$ demonstrated the same large diatropic ring currents that were observed for **19**, with the internal CH showing up near −7 ppm (again some variation was noted with changes in concentration). Three of the *meso*-protons were observed as singlets between 9.4 and 9.7 ppm, but CH-20 was further deshielded by the proximate formyl moiety and resonated near 10.7 ppm. The proton NMR spectrum of **45a** in d_7-DMF showed some small downfield shifts for the external protons, but otherwise was similar to the spectrum obtained in $CDCl_3$. However, the external cyclopentadiene proton CH-3 did show coupling to the internal CH under these conditions and gave a doublet with a coupling constant $^4J = 1.2$ Hz. Addition of trace amounts of TFA to NMR solutions of **45a** in $CDCl_3$ afforded the corresponding monocation **46a** (Scheme 7). This retained the macrocyclic ring current with the interior CH at −5.83 ppm, while the NH's gave rise to three separate resonances at −3.4, −2.3, and −2.2 ppm. Three of the *meso*-protons gave singlets between 9.7 and 10.1 ppm, while the fourth *meso*-proton, CH-20, was again further deshielded and resonated at 10.54 ppm. The external cyclopentadiene proton, CH-3, showed up slightly downfield compared to the free base **45a** at 8.94 ppm. In 50% TFA−$CDCl_3$, the dication **47a** (Scheme 7) was generated and this showed significant differences from the diprotonated forms in the benzocarbaporphyrin series. The internal CH_2 of **47a** gave a resonance at −7.4 ppm, compared to a value of −5.15 for **26a**, and this result suggests that the macrocyclic ring current is significantly larger for this species. The outer cyclopentadiene proton, CH-3, is also deshielded to 11 ppm, while the *meso*-protons show substantial downfield shifts. These data indicate that the fused benzo unit interferes with the macrocyclic ring current in the doubly protonated species giving a greater than 2 ppm upfield shift to the internal methylene group compared to **47**, although macrocyclic aromaticity still dominates the spectroscopic properties for **26** (Scheme 4). Trimethylcarbaporphyrin **45b** shows similar trends to **45a** upon protonation. Of particular note, the cyclopentadiene methyl group of **45b** is observed near 3.5 ppm in the proton NMR spectra for the free base and monocation, but this resonance is deshielded to 4.5 ppm in the dication **47b**. Again, the interior methylene of **47b** is strongly deshielded and resonates at −7.3 ppm. Addition of *d*-TFA to **45a** gave

(43) Lash, T. D.; Denny, C. P. *Tetrahedron* **1995**, *51*, 59. Lash, T. D.; Gandhi, V. *J. Org. Chem.* **2000**, *65*, 8020−8026. Lash, T. D.; Werner, T. M.; Thompson, M. L.; Manley, J. M. *J. Org. Chem.* **2001**, *66*, 3152.

(44) See also: Nguyen, L. T.; Senge, M. O.; Smith, K. M. *J. Org. Chem.* **1996**, *61*, 998.

(45) Richter, D. T.; Lash, T. D. *Tetrahedron Lett.* **1999**, *40*, 6735.

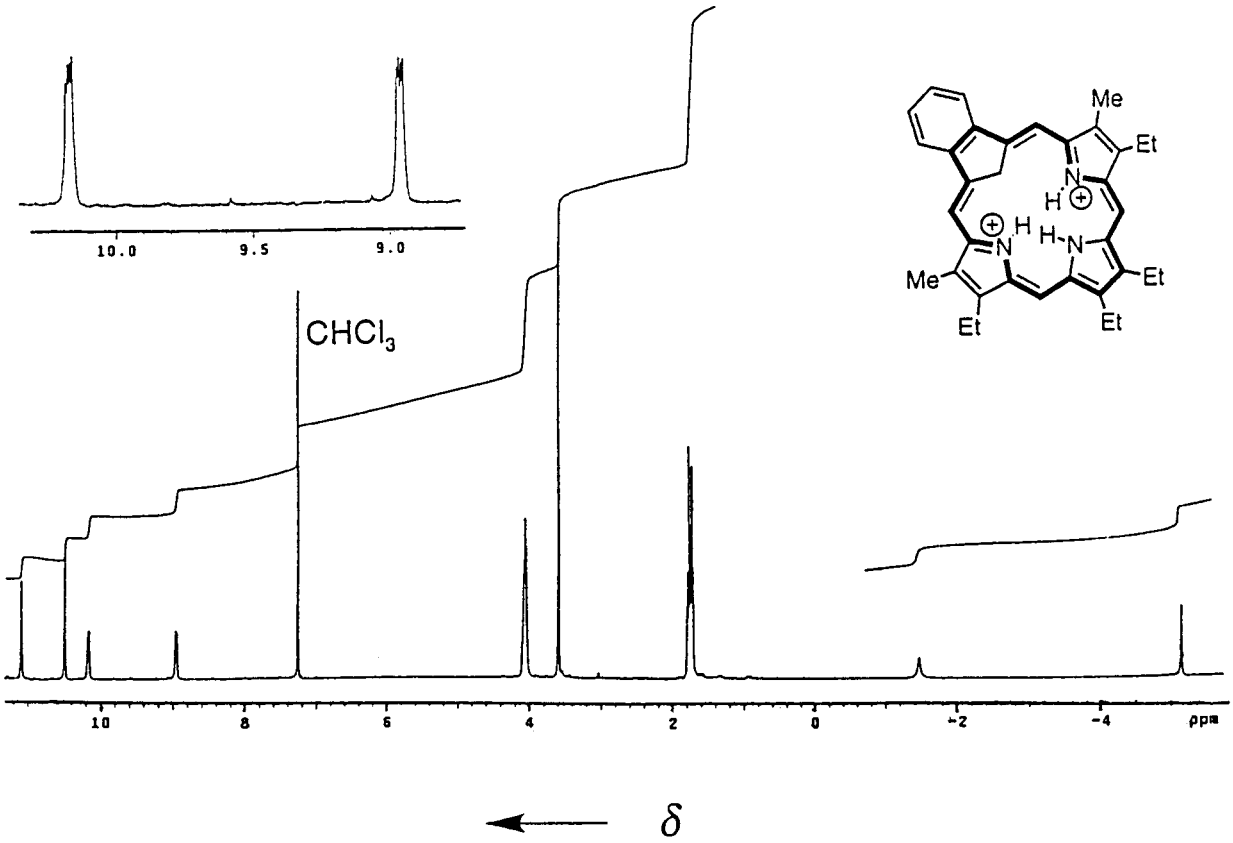

FIGURE 5. 400 MHz proton NMR spectrum of benzocarbaporphyrin **19a** in 50% TFA−$CDCl_3$ at 21 °C. The data shows that C-protonation has occurred to give the dication **26**.

CHART 5

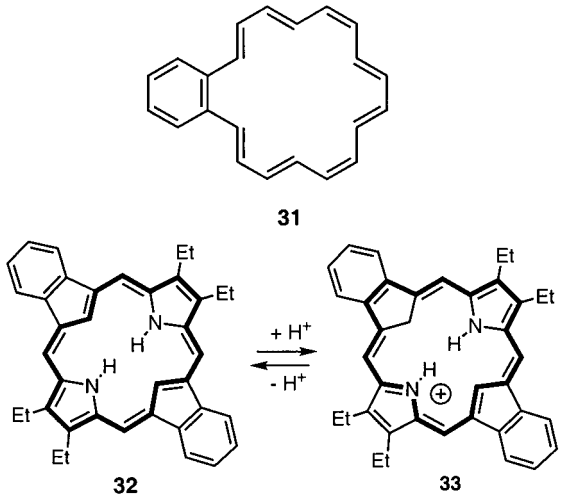

rapid exchange for the NH and internal CH protons. Slow exchange was also observed for the *meso*-protons at positions 10 and 15. In 50% *d*-TFA−$CDCl_3$, after 3 days at room temperature, the resonances for these positions showed a 57−70% loss in intensity, although none of the remaining resonances showed any measurable exchange under these conditions. These results suggest that non-aromatic C-protonated species such as **48** or **49** (or perhaps the related dications) are present in solution in equilibrium with monocation **46** (Scheme 7).

Up to this point, the carbaporphyrin system had not been examined by X-ray crystallographic analysis. How-

CHART 6

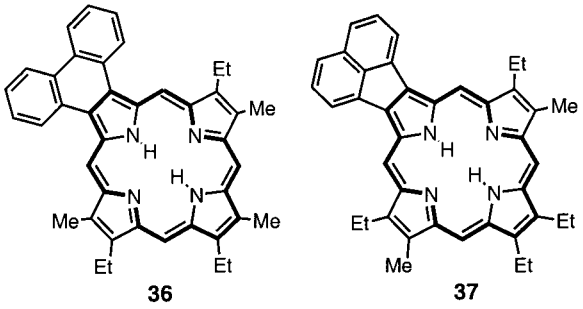

ever, the diphenyl-substituted carbaporphyrin **19b** gave crystals that were suitable for analysis by X-ray diffraction, and the first carbaporphyrin solid state structure is reported below. The molecular structure (Figure 7) shows that the porphyrinoid is reasonably planar as evidenced by the minimal pyrrole to mean macrocycle plane tilts of 2.5°, 4.4°, and 4.9°. The indene subunit, however, is significantly tilted 15.5° out of the mean macrocyclic plane. This presumably relieves steric crowding in the central cavity due to the presence of three hydrogen atoms. All C−N bond distances are equivalent with an average length equal to 1.371(4) Å. The C(6)−N(22)−C(9) and C(16)−N(24)−C(19) bond angles, 111.2-(3)° and 110.9(3)°, respectively, are similarly equivalent; however, the 105.3(3)° C(11)−N(23)−C(14) bond angle is significantly compressed, and this may be attributed to the presence of the nonbonding pair of electrons on N(23). Thus, the three hydrogen atoms, H21, H22, and H24, located in the carbaporphyrin cavity, are attached to the

SCHEME 6

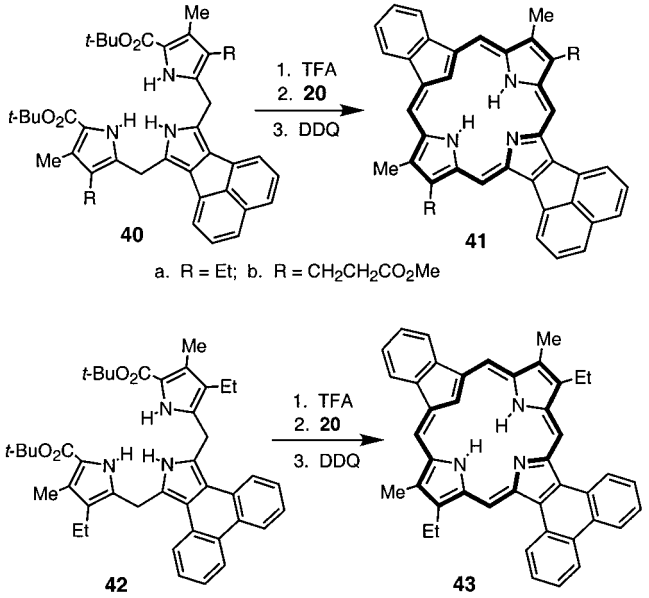

SCHEME 7

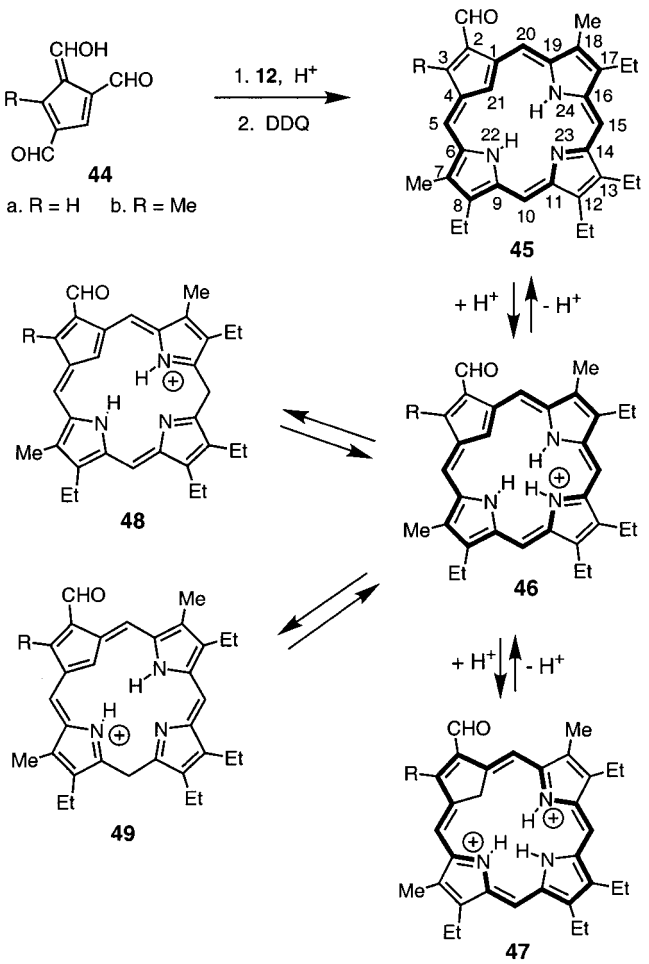

parent atoms C(21), and N(22) and N(24), the pyrrole nitrogens cis to C(21). Located by a difference Fourier immediately following anisotropic refinement of all non-hydrogen atoms, H21, H22, and H24 were allowed to freely refine through the remainder of the structure refinement procedure. The three core hydrogen atoms remained associated with their respective parents, lending further support for the structural assignment. Both solution NMR data and solid-state diffraction data are consistent with tautomer **19b**, which has two NHs flanking the pyrrolene nitrogen, rather than tautomers such as **27b** (Chart 4). This result is in agreement with theoretical studies by Ghosh and co-workers that indicate that tautomers such as **19b** are favored over the alternative forms by approximately 6 kcal/mol.[33] As would be expected, the phenyl groups are tilted 58° out of the carbaporphyrin plane and therefore do not significantly contribute their π systems to the macrocycle.

Electrochemical studies were also performed on carbaporphyrin **19a**. The cyclic voltammogram **19a** is shown in Figure 8. Starting at −0.2 V and scanning in a negative direction, two cathodic waves were observed corresponding to quasi-reversible couples at $E_{1/2} = -1.69$ V and −2.04 V. Scanning positively, five anodic waves were observed, corresponding to irreversible peaks at $E_{p,a} = 0.48$ and 0.68 V, quasi-reversible couples at $E_{1/2} = 0.77$ V and $E_{1/2} = 1.17$ V, as well as a reversible couple at $E_{1/2} = 1.49$ V. These data indicate more complex redox behavior than has been observed for the well studied tetraphenylporphyrin or H_2OEP.[46,47] For example, porphyrins such as H_2OEP display four reversible couples, two oxidative and two reductive couples,[46,47] whereas **19a** displays at least five oxidative and two reductive couples. Due to the complexity of these data, we decided to focus on the reductive processes.

As mentioned above, the free base carbaporphyrin displays two quasi-reversible reductive couples in the cyclic voltammogram at $E_{1/2} = -1.69$ V and −2.04 V ($\Delta E_{1/2} = 0.35$ V). Reductively **19a** looks most similar to porphyrins and metalloporphyrins which display two reversible reductive couples with $\Delta E_{1/2} = 0.42 \pm 0.05$ V.[46,47] The cyclic voltammogram of N-confused porphyrin contains only one irreversible reductive wave in the region scanned.[48] Notably, the difference between the first oxidative couple and the first reductive couple of the free base carbaporphyrin, typically referred to as the HOMO−LUMO gap, falls within the range of free base porphyrins. Compound **19a** has a HOMO−LUMO gap of 2.17 V, whereas an average HOMO−LUMO gap of 2.25 ± 0.15 V for porphyrin and metalloporphyrin complexes has been reported.[46,47]

Conclusions

The synthesis of nine examples of monocarbaporphyrins by the "3 + 1" version of the MacDonald condensation has been completed. These porphyrin analogues retain porphyrin-like electronic spectra and show strong diamagnetic ring currents by proton NMR spectroscopy. Ring fusion of benzo, phenanthro, and acenaphtho units produce increasing bathochromic shifts in that order for UV−vis absorption spectra in parallel with previous results for tetrapyrrolic porphyrins. In addition to spectroscopic characterization, carbaporphyrins have been

(46) Kadish, K. M.; Van Caemelbecke, E.; Royal, G. In *The Porphyrin Handbook*; Kadish, K. M.; Smith, K. M.; Guilard, R., Eds.; Academic Press: San Diego, 2000; Vol. 8, pp 1−114.
(47) Davis, D. G. In *The Porphyrins*; Dolphin, D., Ed.; Academic Press: New York, 1978; Vol. 5.
(48) Furuta, H.; Ogawa, T.; Uwatoko, Y.; Araki, K. *Inorg. Chem.* **1999**, *38*, 2676.

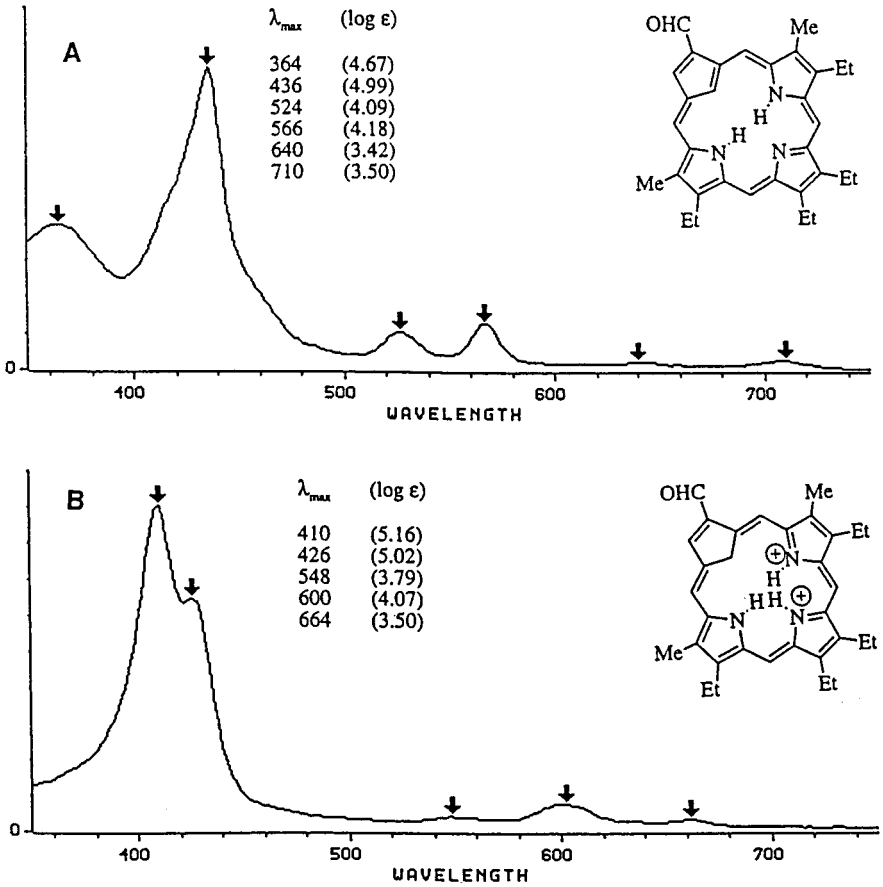

FIGURE 6. UV−vis spectra of formylcarbaporphyrin **45a**. A. Free base in 1% triethylamine−chloroform. B. Dication **47** in 50% TFA−chloroform.

characterized electrochemically and by X-ray crystallography for the first time. Further, protonation studies demonstrate that monoprotonation occurs at low concentrations of TFA, but complex mixtures of different species are generated above 0.1% TFA−CH_2Cl_2. At much higher acid concentrations (50% TFA−chloroform) C-protonated dications are favored. This study provides the foundations for detailed investigations into the synthesis and chemistry of carbaporphyrin systems.

Experimental Section

Triformylcyclopentadienes **44** were synthesized according to the procedure of Hafner et al.;[49] tripyrranes **24a**, **24c**, **40**, and **42** were prepared as described previously.[16,41] EI and FAB mass spectral determinations were made at the Mass Spectral Laboratory, School of Chemical Sciences, University of Illinois at Urbana−Champaign, supported in part by a grant from the National Institute of General Medical Sciences (GM 27029). Elemental analyses were obtained from the School of Chemical Sciences Microanalysis Laboratory at the University of Illinois.

1,3-Diformylindene (20). Prepared by the procedure of Arnold.[50] Recrystallization from acetonitrile−water gave the dialdehyde as brown crystals, mp 198−200 °C (lit. mp 198−200 °C); ^{1}H NMR (d_6-DMSO): δ 7.22 (2H, m), 7.76 (1H, s), 7.96 (2H, m), 9.08 (2H, br s); EI MS (70 eV): *m/z* (rel int.) 172 (M^+; 64%), 171 (14%), 144 (39%), 115 (100%); HRMS: Calcd for $C_{11}H_8O_2$: 172.0524. Found: 172.0524.

8,12,13,17-Tetraethyl-7,18-dimethylbenzo[*b*]-21-carbaporphyrin (19a). Tripyrrane dicarboxylic acid **20a** (100 mg) was stirred with TFA (1 mL) under an atmosphere of nitrogen for 10 min. Dichloromethane (19 mL) was added, followed immediately by 1,3-diformylindene (38 mg), and the mixture was stirred under nitrogen for a further 2 h. The mixture was neutralized by the dropwise addition of triethylamine, DDQ (50 mg) was added, and the resulting solution was stirred for an additional 1 h. The mixture was washed with water and chromatographed on neutral Grade 3 alumina eluting with dichloromethane, and a dark brown fraction was collected. Further chromatography on a silica column, eluting with dichloromethane, gave the product as a broad brown band. Recrystallization from chloroform−methanol afforded the carbaporphyrin **19a** (47 mg; 43%) as fluffy copper-bronze colored crystals, mp >270 °C; UV−vis (1% Et_3N−$CHCl_3$): λ_{max} (log ϵ) 376 (4.63), 424 (5.25), 510 (4.27), 544 (4.21), 602 (3.79), 662 nm (3.25); UV−vis (CH_2Cl_2): λ_{max} (log ϵ) 375 (4.66), 423 (5.23), 510 (4.21), 544 (4.21), 604 (3.77), 662 nm (3.28); UV−vis (0.01% TFA-CH_2Cl_2; monocation **27a**): λ_{max} (log ϵ) 307 (4.54), 399 (4.80), 437 (5.03), 473 (4.56), 550 (4.09), 586 (3.935), 611 nm (3.96); UV−Vis (50% TFA−$CHCl_3$; dication **26a**): λ_{max} (log ϵ) 348 (4.54), 426 (5.27), 462 (sh) (4.47), 614 (3.91), 662 nm (4.42); ^{1}H NMR (500 MHz, $CDCl_3$): δ −6.74 (1H, s), −4.0 (2H, v br), 1.85 (6H, t), 1.87 (6H, t), 3.68 (6H, s), 3.97 (4H, q), 4.07 (4H, q), 7.74 (2H, m), 8.83 (2H, m), 9.82 (2H, s), 10.10 (2H, s); ^{1}H NMR (400 MHz, d_7-DMF): δ −6.78 (1H, s), −3.92 (2H, br s), 1.83−1.88 (12H, 2 overlapping triplets), 3.73 (6H, s), 4.04 (4H, q, J = 7.5 Hz), 4.17 (4H, q, J = 7.5 Hz), 7.77−7.80 (2H, m), 9.14−9.17 (2H, m), 10.04 (2H, s), 10.51 (2H, s); ^{1}H NMR (400 MHz, trace TFA−$CDCl_3$, monocation **27a**: δ −6.75 (1H, s), −4.61 (1H, s), −3.22 (2H, s), 1.69 (6H, t, J = 7.6 Hz), 1.85 (6H, t, J = 7.6 Hz), 3.57 (6H, s), 4.03−4.14 (8H,

(49) Hafner, K.; Vöpel, K. H.; Ploss, G.; König, C. *Liebigs Ann. Chem.* **1963**, *661*, 52.
(50) Arnold, Z. *Coll. Czech. Chem. Commun.* **1965**, *30*, 2783.

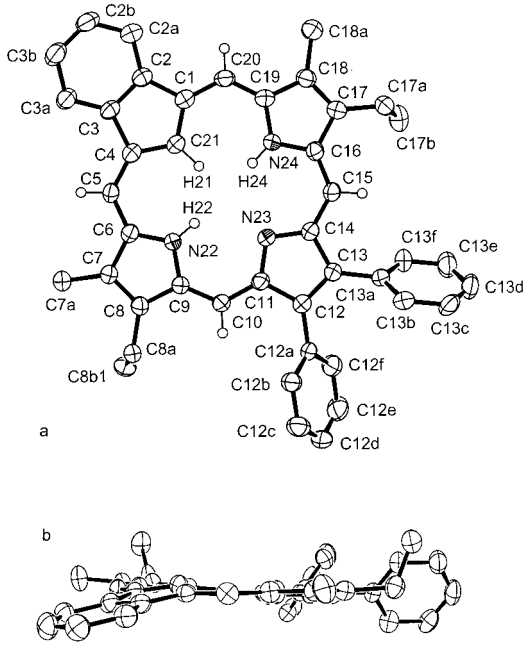

FIGURE 7. (A) Aerial view ORTEP drawing with shaded ellipsoids of **19b** showing the atom labeling scheme. Non-hydrogen atoms are represented by Gaussian ellipsoids at the 50% probability level. Hydrogen atoms have been omitted for clarity with the exception of the carbaporphyrin core hydrogen atoms that have been drawn arbitrarily small. (B) Edge view ORTEP drawing of **19b**.

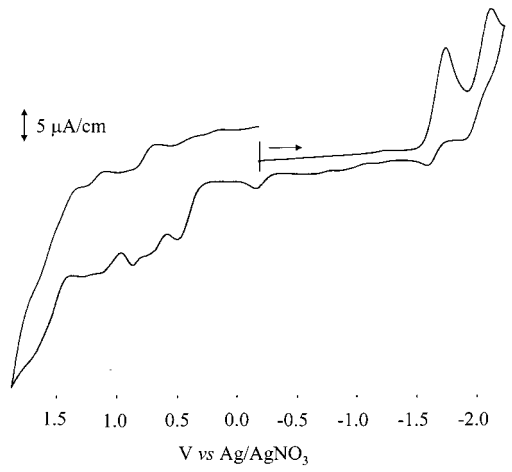

FIGURE 8. Cyclic voltammogram of **19a** in 0.2 M Bu_4NBF_4/CH_2Cl_2.

2 overlapping quartets), 7.71−7.74 (2H, m), 8.68−8.71 (2H, m), 10.06 (2H, s), 10.33 (2H, s); ^{1}H NMR (400 MHz, 50% TFA−$CDCl_3$, dication **26a**, 20 °C): δ −5.15 (2H, s), −1.47 (2H, br s), 1.74 (6H, t, J = 7.8 Hz), 1.78 (6H, t, J = 7.8 Hz), 3.60 (6H, s), 4.02−4.10 (8H, m), 8.94−8.98 (2H, m), 10.15−10.18 (2H, m), 10.45 (2H, s), 11.10 (2H, s); ^{1}H NMR (400 MHz, 50% TFA−$CDCl_3$, dication **26a**, −10 °C): δ −5.21 (2H, s), −1.6 (1H, vb), −1.55 (2H, s), 1.67 (6H, t, J = 7.6 Hz), 1.73 (6H, t, J = 7.8 Hz), 3.57 (6H, s), 4.00−4.08 (8H, m), 8.94−8.96 (2H, m), 10.14−10.17 (2H, m), 10.46 (2H, s), 11.07 (2H, s); ^{13}C NMR ($CDCl_3$): δ 11.4, 17.4, 18.6, 19.6, 20.0, 95.5, 98.8, 109.7, 120.6, 126.6, 132.5, 133.9, 135.6, 137.8, 141.6, 144.6, 152.9; ^{13}C NMR (50% TFA−$CDCl_3$, dication **26a**): δ 11.1, 16.1, 17.2, 20.1, 20.3, 32.9, 107.8, 108.2, 125.2, 134.9, 138.0, 139.5, 140.6, 146.0, 146.5, 150.9, 151.7; EI MS: *m*/*z* (rel int.) 501 (7.5), 500 (41), 499 (100; M^+), 498 (3.4), 497 (3.7) 496 (9.1), 484 (6.4), 469 (3.4), 454 (3.5), 249.8 (17; M^{2+}); HRMS (EI): calcd for $C_{35}H_{37}N_3$: *m*/*z* 499.29795; found: 499.29875. Anal. Calcd for $C_{35}H_{37}N_3 \cdot H_2O$: calcd C, 83.38; H, 7.49; N, 8.33. Found: C, 83.31; H, 7.29; N, 8.19.

8,12,13,17-Tetraethyl-2-formyl-7,18-dimethyl-21-carbaporphyrin (45a). Formylcarbaporphyrin **45a** was prepared by the procedure outlined above from tripyrrane **24a** (100 mg) and triformylcyclopentadiene **44a** (33 mg). Recrystallization from chloroform−methanol yielded the title porphyrinoid (7 mg; 7.7%) as purple crystals, mp >240 °C. UV−vis (1% Et_3N−CH_2Cl_2): λ_{max} (log ϵ) 364 (4.67), 436 (4.99), 524 (4.09), 566 (4.18), 640 (3.42), 710 nm (3.50); UV−vis (CH_2Cl_2): λ_{max} (log ϵ) 362 (4.71), 434 (4.99), 524 (4.085), 564 (4.16), 643 (3.37), 707 nm (3.44); UV−vis (0.01% TFA-CH_2Cl_2; monocation **46a**): λ_{max} (log ϵ) 316 (4.53), 394 (4.775), 424 (4.84), 434 (4.84), 445 (4.86), 491 (4.15), 550 (4.01), 591 (3.72), 713 nm (3.20); UV−vis (50% TFA−$CHCl_3$; dication **47a**): λ_{max} (log ϵ) 410 (5.16), 426 (5.02), 548 (3.79), 600 (4.07), 664 nm (3.50); ^{1}H NMR (500 MHz, $CDCl_3$): δ −6.80 (1H, s), −3.80 (2H, v br), 1.79 (12H, m), 3.43 (3H, s), 3.53 (3H, s), 3.81 (4H, q), 3.92 (4H, 2 overlapping quartets), 8.60 (1H, s), 9.40 (1H, s), 9.46 (1H, s), 9.48 (1H, s), 10.66 (1H, s), 10.69 (1H, s); ^{1}H NMR (400 MHz, d_7-DMF): δ −6.49 (1H, s), −3.47 (2H, s), 1.79−1.84 (12H, 2 overlapping triplets), 3.59 (3H, s), 3.60 (3H, s), 3.96 (4H, q, J = 7.7 Hz), 4.10 (4H, q, J = 7.7 Hz), 9.11 (1H, d, J = 1.2 Hz), 9.85 (1H, s), 9.87 (1H, s), 10.17 (1H, s), 10.82 (1H, s), 10.85 (1H, s); ^{1}H NMR (400 MHz, trace TFA−$CDCl_3$, monocation **46a**): δ −5.83 (1H, s), −3.38 (1H, br), −2.31 (1H, s), −2.23 (1H, s), 1.66 (6H, t), 1.80 (6H, t), 3.48 (3H, s), 3.50 (3H, s), 3.93−4.04 (8H, m), 8.94 (1H, s), 9.77 (1H, s), 9.81 (1H, s), 10.06 (1H, s), 10.54 (1H, s), 10.96 (1H, s); ^{1}H NMR (400 MHz, 50% TFA−$CDCl_3$, dication **47a**): δ −7.42 (2H, s), −3.67 (2H, br), 1.77−1.85 (12H, m), 3.76 (3H, s), 3.77 (3H, s), 4.20−4.28 (8H, m), 10.99 (1H, s), 11.05 (1H, s), 11.50 (1H, s), 11.60 (1H, s), 11.92 (1H, s), 12.12 (1H, s); ^{13}C NMR ($CDCl_3$): δ 11.2, 11.4, 17.1, 17.2, 18.3, 19.4, 19.9, 94.3, 95.0, 104.1, 106.8, 108.4, 132.7, 133.0, 134.9, 135.3, 135.7, 135.9, 136.7, 137.7, 137.8, 138.5, 138.9, 143.3, 145.3, 145.6, 155.5, 155.8, 189.3; EI MS: *m*/*z* (rel int.) 479 (8), 478 (37), 477 (100; M^+), 476 (2.4), 462 (4.2), 238.8 (11.5; M^{2+}); HRMS (EI): calcd for $C_{32}H_{35}N_3O$: 477.2780 *m*/*z*; found: 477.2780.

8,12,13,17-Tetraethyl-2-formyl-3,7,18-trimethyl-21-carbaporphyrin (45b). Carbaporphyrin **45b** was prepared as outlined for **19a** from tripyrrane **24a** (100 mg) and methyltriformylcyclopentadiene **44b** (33 mg). Recrystallization from chloroform−methanol gave formylcarbaporphyrin **45b** (7.0 mg, 6.5%) as purple crystals, mp > 240 °C. UV−vis (1% Et_3N−CH_2Cl_2): λ_{max} (log ϵ) 368 (4.69), 438 (4.89), 528 (4.09), 566 (4.12), 642 (3.43), 710 nm (3.30); UV−vis (0.01% TFA-CH_2Cl_2; monocation **46b**): λ_{max} (log ϵ) 321 (4.49), 401 (4.84), 428 (4.79), 447 (sh, 4.72), 500 (sh, 4.01), 551 (3.96), 593 (3.77), 647 (3.58), 708 nm (3.31); UV−vis (50% TFA−$CHCl_3$; dication **47b**): λ_{max} (log ϵ) 414 (5.26), 428 (5.07), 554 (3.73), 604 (4.04), 664 nm (3.75); ^{1}H NMR (400 MHz, $CDCl_3$): δ −6.62 (1H, s), −3.52 (2H, br s), 1.77−1.85 (12H, m), 3.51 (3H, s), 3.56 (3H, s), 3.57 (3H, s), 3.87 (4H, q), 3.94−4.01 (4H, 2 overlapping quartets), 9.54 (1H, s), 9.61 (1H, s), 9.71 (1H, s), 10.78 (1H, s), 11.00 (1H, s); ^{1}H NMR (400 MHz, trace TFA−$CDCl_3$, monocation **46b**): δ −6.07 (1H, s), −3.27 (1H, br s), −1.99 (1H, s), −1.91 (1H, s), 1.62−1.68 (6H, 2 overlapping triplets), 1.81 (6H, t), 3.47 (6H, s), 3.59 (3H, s), 3.92−4.03 (8H, m), 9.74 (1H, s), 9.82 (1H, s), 10.04 (1H, s), 10.75 (1H, s), 10.99 (1H, s); ^{1}H NMR (400 MHz, 50% TFA−$CDCl_3$, dication **47b**): δ −7.28 (2H, s), −3.48 (2H, br), 1.76−1.85 (12H, m), 3.73 (3H, s), 3.75 (3H, s), 4.15−4.27 (8H, m), 4.53 (3H, s), 10.86 (1H, s), 10.97 (1H, s), 11.46 (1H, s), 11.97 (1H, s), 12.05 (1H, s); ^{13}C NMR ($CDCl_3$): δ 11.3, 11.5, 17.2, 17.3, 18.4, 19.5, 19.9, 94.3, 95.5, 102.2, 103.7, 107.9, 131.6, 133.8, 134.0, 134.6, 135.2, 135.4, 135.6, 137.5, 137.8, 138.7, 145.0, 145.5, 152.9, 154.9, 155.6, 188.2; EI MS: *m*/*z* (rel int.) 493(9), 492 (35), 491 (100; M^+), 490 (2.8), 476 (4.2) 464 (3.5), 463 (6.3), 462 (5.1), 245.7 (6.9; M^{2+}); HRMS (EI): calcd for $C_{33}H_{37}N_3O$: *m*/*z* 491.2937. Found: 491.2937.

12,13-Butano-8,17-diethyl-7,18-dimethylbenzo[*b*]-21-carbaporphyrin (**19c**). Butanobenzocarbaporphyrin **19c** was prepared in the same procedure as **19a** from tripyrrane **24c** (200 mg) and 1,3-diformylindene (75 mg). Recrystallization from chloroform−methanol afforded **19c** (104 mg; 50.5%) as purple-colored crystals, >300 °C; UV−vis (1% Et_3N−CH_2Cl_2): λ_{max} (log ϵ) 376 (4.63), 426 (5.24), 512 (4.26), 544 (4.16), 602 (3.71), 662 nm (3.28); UV−vis (50% TFA−$CHCl_3$; **26c**): λ_{max} (log ϵ) 346 (4.56), 424 (5.27), 616 (3.92), 672 nm (4.47); ^{1}H NMR (300 MHz, $CDCl_3$): δ −6.80 (1H, s), −4.0 (2H, v br), 1.83 (6H, t), 2.47 (4H, m), 3.61 (6H, s), 4.04 (8H, m), 7.75 (2H, m), 8.82 (2H, m), 9.64 (2H, s), 10.06 (2H, s); ^{1}H NMR (300 MHz, 50% TFA−$CDCl_3$; dication **26c**): δ −5.12 (2H, br s), −1.20 (2H, br s), 1.77 (6H, t), 2.49 (4H, br m), 3.59 (6H, s), 4.05 (8H, m), 8.96 (2H, m), 10.16 (2H, m), 10.41 (2H, s), 11.11 (2H, s); ^{13}C NMR ($CDCl_3$): δ 11.4, 17.3, 19.6, 23.8, 24.2, 95.2, 98.9, 109.8, 120.7, 126.7, 132.6, 133.9, 135.5, 135.8, 137.7, 141.8, 141.9, 153.3; ^{13}C NMR (50% TFA−$CDCl_3$; dication **26c**): δ 11.1, 16.1, 20.3, 22.6, 23.5, 32.8, 107.7, 108.3, 125.2, 135.0, 138.4, 139.7, 141.1, 143.7, 146.2, 151.0, 151.4 (2); EI MS: *m*/*z* (rel int.) 499 (8), 498 (38), 497 (100; M^+), 496 (3.0), 482 (8.0; $[M - CH_3]^+$), 469 (1.6; $[M - CH_2{=}CH_2]^+$), 454 (2.4), 248.8 (18; M^{2+}); HRMS (EI): calcd for $C_{35}H_{35}N_3$: *m*/*z* 497.2831. Found: 497.2827.

8,17-Diethyl-7,18-dimethyldibenzo[*b*,*l*]-21-carbaporphyrin (**38**)**.** Butanobenzocarbaporphyrin **19c** (11 mg) and DDQ (11 mg) were stirred under reflux with 10 mL of toluene for 2 h. The solvent was removed under reduced pressure and the residue dissolved in CH_2Cl_2. The solution was washed with water and chromatographed on a silica column eluting with CH_2Cl_2. Recrystallization from chloroform−methanol gave **38** (8.0 mg; 46%) as fluffy copper-bronze-colored crystals, mp > 300 °C; UV−vis (1% Et_3N−CH_2Cl_2): λ_{max} (log ϵ) 386 (4.66), 432 (5.27), 452 (sh) (4.49), 518 (4.24), 552 (4.43), 610 (3.86), 672 nm (3.91); UV−vis (50% TFA−$CHCl_3$): λ_{max} (log ϵ) 370 (4.57), 438 (5.08), 486 (sh) (4.43), 728 nm (4.43); ^{1}H NMR (300 MHz, $CDCl_3$): δ −6.59 (1H, s), −4.02 (2H, br s), 1.87 (6H, t), 3.61 (6H, s), 4.07 (4H, q), 7.76 (2H, m), 8.06 (2H, m), 8.81 (2H, m), 9.26 (2H, m), 10.04 (2H, s), 10.06 (2H, s); ^{1}H NMR (300 MHz, TFA−$CDCl_3$): δ −6.01 (2H, br s), −2.30 (3H, v br s, 3 x NH), 1.83 (6H, t), 3.72 (6H, s), 4.18 (4H, q), 8.55 (2H, m), 9.01 (2H, m), 9.60 (2H, m), 10.29 (2H, m), 11.03 (2H, s), 11.40 (2H, s); ^{13}C NMR ($CDCl_3$): δ 11.9, 16.5, 20.3, 96.2, 96.6, 123.7, 123.8, 131.6, 131.6, 134.0, 134.1, 137.5, 139.4, 139.5, 141.9, 142.7, 144.0; EI MS: *m*/*z* (rel int.) 495 (7.4), 494 (39), 493 (100; M^+), 492 (3.7), 491 (3.6), 478 (20; $[M - CH_3]^+$); 463 (3.4), 462 (3.3), 247 (16; M^{2+}); HRMS (EI): calcd for $C_{35}H_{31}N_3$: *m*/*z* 493.2518. Found: 493.2517.

8,17-Diethyl-7,18-dimethylacenaphtho[*b*]benzo[*l*]-21-carbaporphyrin (41a). Tripyrrane **40a** was stirred with TFA (1.0 mL) for 10 min under nitrogen. Dichloromethane (19 mL) was added, followed immediately by diformylindene **20** (27 mg), and the resulting solution was stirred under N_2 in the dark for a further 2 h. The solution was neutralized with triethylamine, DDQ (36 mg) was added, and the mixture stirred for 1 h. The mixture was diluted with dichloromethane, washed with water, and evaporated under reduced pressure. The residue was columned on Grade III neutral alumina, eluting first with dichloromethane, and then chloroform with increasing amounts of methanol (0−5%). The product fraction was recrystallized from chloroform−methanol to give the acenaphthocarbaporphyrin (16 mg; 18%) as a dark blue solid, mp > 300 °C; UV−vis (1% Et_3N−$CHCl_3$): λ_{max} (log ϵ) 402 (4.63), 456 (5.07), 511 (4.00), 546 (4.01), 590 (4.60), 624 (4.10), 688 nm (3.21); UV−vis (50% TFA−$CHCl_3$): λ_{max} (log ϵ) 307 (4.24), 368 (4.53), 474 (5.23), 632 (4.17), 691 nm (4.35); ^{1}H NMR (400 MHz, 50% TFA−$CDCl_3$): δ −4.64 (2H, br s), −1.0 (2H, br s), 1.90 (6H, t, J = 7.6 Hz), 3.63 (6H, s), 4.15 (4H, q, J = 7.6 Hz), 8.16 (2H, t, J = 7 Hz), 8.38 (2H, d, 7.9 Hz), 8.96 (2H, m), 9.07 (2H, d, J = 6.7 Hz), 10.14 (2H, m), 10.89 (2H, s), 11.02 (2H, s); ^{13}C NMR (50% TFA−$CDCl_3$): δ 11.0, 16.1, 20.3, 33.1, 107.8, 109.6, 124.9, 126.8, 129.5, 130.3, 131.5, 131.7, 134.6, 134.7, 137.8, 137.9, 139.4, 145.4, 145.7, 150.9, 151.7; HRMS (FAB): calcd for $C_{41}H_{33}N_3$ + H: *m*/*z* 568.2753; found: 568.2753.

8,17-Bis(2-methoxycarbonylethyl)-7,18-dimethylacenaphtho[*b*]benzo[*l*]-21-carbaporphyrin (41b). The title carbaporphyrin was prepared by the foregoing procedure from tripyrrane **40b** (100 mg), **20** (23 mg), and DDQ (30 mg). Recrystallization from chloroform−methanol gave the carbaporphyrin (26 mg; 29%) as a dark blue solid, mp > 300 °C; UV−vis (1% Et_3N−$CHCl_3$): λ_{max} (log ϵ) 343 (4.23), 395 (4.57), 454 (5.02), 509 (4.00), 544 (3.96), 587 (4.49), 624 nm (3.99); UV−vis (50% TFA−$CHCl_3$): λ_{max} (log ϵ) 307 (4.20), 371 (4.42), 476 (5.13), 640 (4.08), 702 nm (4.22); ^{1}H NMR (400 MHz, $CDCl_3$): δ −7.67 (1H, s), −5.2 (2H, br s), 3.07 (4H, t, J = 7.6 Hz), 3.42 (6H, s), 3.60 (6H, s), 4.11 (4H, t, J = 7.6 Hz), 7.83−7.85 (2H, m), 7.97 (2H, t, J = 7 Hz), 8.06 (2H, d, J = 8.5 Hz), 8.66 (2H, d, J = 6.7 Hz), 8.78−8.81 (2H, m), 9.46 (2H, s), 9.70 (2H, s); ^{1}H NMR (400 MHz, 50% TFA−$CDCl_3$): δ −4.97 (2H, br s), 3.34 (4H, t, J = 7.6 Hz), 3.65 (6H, s), 3.81 (6H, s), 4.51 (4H, br t), 8.16 (2H, t, J = 7 Hz), 8.38 (2H, d, J = 7.9 Hz), 8.97 (2H, m), 9.18 (2H, d, J = 6.7 Hz), 10.14 (2H, m), 11.04 (4H, s); HRMS (FAB): calcd for $C_{45}H_{37}N_3O_4$ + H: *m*/*z* 684.2862; found: 684.2861.

8,17-Diethyl-7,18-dimethylbenzo[*b*]phenanthro[*l*]-21-carbaporphyrin (43). The title compound was prepared from tripyrrane **42** (100 mg), **20** (26 mg) and DDQ (35 mg) by the foregoing procedure. Chromatography on Grade III alumina, eluting with CH_2Cl_2, followed by chromatography on silica eluting with CH_2Cl_2, gave the product as a brown fraction. Recrystallization from chloroform−methanol gave the phenanthrocarbaporphyrin (25 mg; 28%) as a flaky dark burgandy-colored solid, mp > 300 °C; UV−vis (1% Et_3N−$CHCl_3$): λ_{max} (log ϵ) 390 (4.64), 442 (5.30), 496 (4.26), 529 (4.13), 568 (4.49), 618 (3.93), 677 nm (3.44); UV−vis (50% TFA−$CHCl_3$): λ_{max} (log ϵ) 355 (4.45), 462 (5.08), 606 (3.94), 638 (4.07), 698 nm (4.34); ^{1}H NMR (400 MHz, $CDCl_3$): δ −7.12 (1H, s), −4.8 (2H, br s), 1.74 (6H, t, J = 7.6 Hz), 3.46 (6H, s), 3.90 (4H, q, J = 7.6 Hz), 7.77−7.79 (2H, m), 7.92 (2H, t, J = 7.3 Hz), 8.10 (2H, t, J = 7.3 Hz), 8.74−8.76 (2H, m), 9.09 (2H, d, J = 8.5 Hz), 9.73 (2H, d, J = 8.5 Hz), 9.77 (2H, s), 10.36 (2H, s); ^{1}H NMR (400 MHz, 50% TFA−$CDCl_3$): δ −4.40 (2H, s), 0.05 (2H, br s), 1.76 (6H, t, J = 7.6 Hz), 3.51 (6H, s), 4.01 (4H, q, J = 7.6 Hz), 8.20 (2H, t, J = 7.3 Hz), 8.28 (2H, t, J = 7.3 Hz), 8.91−8.93 (2H, m), 9.25 (2H, d, J = 8.5 Hz), 9.58 (2H, d, J = 7.9 Hz), 10.06−10.08 (2H, m), 10.86 (2H, s), 11.10 (2H, s); ^{13}C NMR (50% TFA−$CDCl_3$): δ 11.0, 15.9, 20.3, 33.7, 107.9, 108.7, 124.9, 125.2, 126.6, 127.2, 129.7, 130.3, 133.7, 134.5, 136.4 (2), 137.1, 139.7, 145.4, 149.8, 152.1, 152.6; HRMS (FAB): calcd for $C_{43}H_{35}N_3$ + H: *m*/*z* 594.2909; found: 594.2910.

2,5-Bis(5-benzyloxycarbonyl-3-ethyl-4-methyl-2-pyrrolylmethyl)-3,4-diphenylpyrrole (21b). A stirred mixture of benzyl 5-acetoxymethyl-4-ethyl-3-methylpyrrole-2-carboxylate[51] (1.45 g) and 3,4-diphenylpyrrole[52] (0.50 g) in acetic acid (2 mL) and ethanol (300 mL) was heated under reflux under a nitrogen atmosphere for 16 h. The solution was cooled to room temperature and further chilled with an ice bath. The resulting precipitate was suction-filtered, washed with cold ethanol, and dried in vacuo to give the tripyrrane dibenzyl ester (1.21 g; 73%) as an off-white powder, mp 135 °C; ^{1}H NMR (400 MHz, $CDCl_3$): δ 0.74 (6H, t, J = 7.4 Hz), 2.01 (4H, q), 2.21 (6H, s), 3.75 (4H, br s), 4.52 (4H, br s), 7.05−7.08 (8H, m), 7.16 (2H, t, J = 7.2 Hz), 7.22 (4H, d, J = 7.6 Hz), 7.25−7.27 (6H, m), 9.39 (1H, br s), 11.35 (2H, br s); ^{13}C ($CDCl_3$): δ 11.2, 15.7, 17.1, 22.8, 65.6, 117.6, 120.1, 123.9, 125.3, 125.4, 126.8, 127.0, 127.6, 128.0, 128.3, 128.5, 130.5, 132.7, 136.5, 137.0, 163.1. Anal. Calcd for $C_{48}H_{47}N_3O_4$: calcd C, 78.95; H, 6.49; N, 5.76. Found: C, 78.98; H, 6.43; N, 5.89.

8,17-Diethyl-7,18-dimethyl-12,13-diphenylbenzo[*b*]-21-carbaporphyrin (19b). The foregoing dibenzyl ester (1.52 g)

(51) Johnson, A. W.; Kay, I. T.; Markham, E.; Price, R.; Shaw, K.B. *J. Chem. Soc.* **1959**, 3416.
(52) Friedman, M. *J. Org. Chem.* **1965**, *30*, 859.

was dissolved in freshly distilled THF (225 mL) in a hydrogenation vessel, methanol (75 mL) and triethylamine (20 drops) were added, and the air was flushed out with a stream of nitrogen. Palladium-charcoal (10%, 300 mg) was added and the resulting mixture shaken under a hydrogen atmosphere at 40 psi overnight. The catalyst was filtered off and the solvent removed under reduced pressure. The resulting residue was taken up in 3% aqueous ammonia and neutralized to a litmus end point while maintaining the temperature of the solution between 0 and 5 °C with the aid of a salt−ice bath. The resulting precipitate was suction-filtered and washed repeatedly with water to remove all traces of water. After being dried overnight in vacuo, the dicarboxylic acid **24b** (1.065 g; 93%) was obtained as a pink powder that was used without further purification. Tripyrrane **24b** (100 mg) was stirred with TFA (2 mL) in a pear-shaped flask for 10 min under nitrogen. The solution was diluted with dichloromethane (38 mL), diformylindene (31 mg) was immediately added, and the solution was stirred in the dark under N_2 for a further 2 h. The solution was neutralized by the dropwise addition of triethylamine, DDQ (50 mg) was added, and the resulting solution was stirred for an additional 1 h. The mixure was washed with water and the solvent removed under reduced pressure. The residue was chromatographed on Grade 3 alumina, eluting with dichloromethane, and the product collected as a brown band. Recrystallization from chloroform−methanol gave the diphenylcarbaporphyrin (53 mg; 51%) as shiny purple crystals, mp > 300 °C; UV−vis ($CHCl_3$): λ_{max} (log ϵ) 430 (5.59), 518 (4.20), 555 (4.36), 605 (3.83), 665 (2.97); UV−vis (CH_2Cl_2): λ_{max} (log ϵ) 385 (4.71), 429 (5.325), 517 (4.27), 553 (4.39), 605 (3.93), 666 nm (3.51); UV−vis (0.01% TFA-CH_2Cl_2; monocation **27b**): λ_{max} (log ϵ) 310 (4.435), 402 (4.75), 443 (5.14), 476 (4.51), 555 (4.03), 595 (4.02), 617 (sh, 3.92), 679 nm (3.29); UV−vis (50% TFA−$CHCl_3$; dication **26b**): λ_{max} (log ϵ) 435 (5.30), 607 (4.01), 661 (4.39); ^{1}H NMR (400 MHz, $CDCl_3$): δ −6.91 (1H, s), −4.07 (2H, br s), 1.75 (6H, t, J = 7.5 Hz), 3.59 (6H, s), 3.91 (4H, q, J = 7.5 Hz), 7.60 (2H, t, J = 7.2 Hz), 7.68 (4H, t, J = 7.4 Hz), 7.73 (2H, m), 7.97 (4H, d, J = 7.6 Hz), 8.78 (2H, m), 9.86 (2H, s), 10.03 (2H, s);^{1}H NMR (400 MHz, trace TFA−$CDCl_3$; monocation **27b**): δ −6.71 (1H, s), −4.29 (1H, br), −3.23 (2H, br), 1.60 (6H, t, J = 7.5 Hz), 3.56 (6H, s), 3.91 (4H, q, J = 7.5 Hz), 7.66−7.75 (8H, m), 7.97 (4H, d, J = 6.8 Hz), 8.68−8.70 (2H, m), 10.11 (2H, s), 10.34 (2H, s); ^{1}H NMR (400 MHz, 50% TFA−$CDCl_3$; dication **26b**): δ −4.67 (2H, s), −0.84 (2H, br s), 1.66 (6H, t, J = 7.6 Hz), 3.53 (6H, s), 3.85 (4H, q, J = 7.6 Hz), 7.72−7.74 (3H, m), 7.79−7.81 (2H, m), 8.89−8.94 (2H, m), 10.07−10.12 (2H, m), 10.31 (2H, s), 10.94 (2H, s); ^{13}C ($CDCl_3$): δ 11.6, 17.3, 19.7, 98.5, 99.1, 110.0, 120.6, 126.8, 127.2, 128.5, 132.5, 132.7, 134.6, 135.6, 136.1, 137.0, 138.7, 141.4, 144.3, 151.1; HRMS (EI): calcd for $C_{43}H_{37}N_3$: 595.2984; found: 595.2987. Anal. Calcd for $C_{43}H_{37}N_3 \cdot H_2O$: calcd C, 84.14; H, 6.40; N, 6.84. Found: C, 84.57; H, 6.13; N, 6.95.

Crystal Structure Determination of 19b. X-ray quality crystals were obtained by the addition of methanol to a hot chloroform solution. A dark blue plate thereby obtained of approximate dimensions 0.34 × 0.16 × 0.10 mm was mounted on a glass fiber with super-glue and transferred to a Brucker P4/R4/SMART 1000 CCD diffractometer.[53] The X-ray diffraction data were collected at −80 °C using Mo Kα radiation. Data collection and cell refinement were performed using SMART.[53a] The unit cell parameters were obtained from a least squares refinement of 2778 centered reflections. The systematic absences indicated the space group P_{-1} (no. 02).[54] Carbaporphyrin **19b** was found to crystallize in the triclinic crystal system with the following cell parameters: a = 10.7457(8) Å, b = 11.8726(9) Å, c = 14.160(1) Å, α = 66.692(2)°, β = 76.363(1)°, and γ = 83.235(2)°, Z = 2. A total of 8081 reflections were collected, of which 6489 were unique, and 3473 were observed $F^2_o > 2\sigma(F^2_o)$. Data reduction was accomplished using SAINT.[53b] The data were corrected for absorption through use of the SADABS procedure.[53c]

Solution and data analysis was performed using the WinGX software package.[55] The structure of **19b** was solved using the direct method program SHELXS-97 and the refinement completed using the program SHELXL-97.[56] With the exception of the three core hydrogen atoms, hydrogen atoms were assigned positions based on the geometries of the attached carbon atoms and were given thermal parameters of 20% greater than the attached atoms. Ethyl carbons, C8b1 and C8b2, represent the same atom disordered over two occupancy sites, 60% and 40%, respectively. Both were, nonetheless, refined anisotropically. The three core hydrogen atoms, H21, H22, and H24, were located by a difference Fourier immediately following anisotropic refinement of all non-hydrogen atoms and were allowed to freely refine through the remainder of the process. Full-matrix least-squares refinement on F^2 led to a convergence with R_1 = 0.065 and wR_2 = 0.141 for 3473 data with $F^2_o > 2\sigma(F^2_o)$. A final difference Fourier synthesis showed features in the range of + 0.334 to −0.294 $e^-/Å^3$. An ORTEP[55b] drawing of the refined structure is shown in Figure 7.

Complete X-ray structural data have been deposited at the Cambridge Crystallographic Data Center CCDC no. 184698. Copies of this information can be obtained free of charge from The Director, CCDC, 12 Union Road, Cambridge CB2 1EZ, UK (Fax: + 44−1223−336033; e-mail: deposit@ccdc.cam.ac.uk or www: http://www.ccdc.cam.ac.uk).

Cyclic Voltammetry. The electrochemical studies were carried out in anhydrous dichloromethane using a BAS CV-27 potentiostat equipped with an $x-y$ recorder. A conventional three-electrode cell consisting of a platinum disk working electrode, a platinum wire auxiliary electrode, and a $Ag/AgNO_3$ (0.01 M) reference electrode was used. The cyclic voltammograms were run in a 0.2 M Bu_4NBF_4 solution in an inert atmosphere glovebox at a scan rate of 200 mV/s. The scanning limits were +2.2 V and −1.9 V vs $Ag/AgNO_3$.

Acknowledgment. This material is based upon work supported by the National Science Foundation under Grant Nos. CHE-9732054 and CHE-0134472, the Petroleum Research Fund, administered by the American Chemical Society, and the Camille and Henry Dreyfus Scholar/Fellow Program. We thank Dr. Robert McDonald and The University of Alberta Structure Determination Laboratory for collecting the experimental data set for the X-ray structure of **19b** and for useful discussions.

Supporting Information Available: UV−vis, ^{1}H NMR, ^{13}C NMR, and mass spectra for selected compounds are provided. Tables of crystallographic details, atomic coordinates, bond lengths and angles, critical angle planes, torsional angles, anisotropic thermal parameters and hydrogen atom parameters for carbaporphyrin **19b** are also available. This material is available free of charge via the Internet at http://pubs.acs.org.

JO020267B

(53) (a) Brucker SMART 1000 CCD software package; Brucker Advanced X-ray Solutions: Madison, WI, 1999. (b) Brucker SAINT Integration Software for Single-Crystal Data frames − h, k, l, intensity; Brucker Advanced X-ray Solutions: Madison, WI, 1999. (c) Brucker SADABS-Empirical adsorption correction procedures; Brucker Advanced X-ray Solutions: Madison, WI, 1999.

(54) McArdle, P. *J. Appl. Crystallogr.* **1996**, *29*, 306.

(55) Farrugia, L. J. *J. Appl. Crystallogr.* **1999**, *32*, 837. b. Farrugia, L. J. *J. Appl. Crystallogr.* **1997**, *30*, 565.

(56) (a) Sheldrick, G. M. *Acta Crystallogr.* **1990**, *A46*, 467. (b) Sheldrick, G. M. *SHELXS-97*; 97−2 ed.; University of Goettingen: Goettingen, Germany, 1997. (c) Sheldrick, G. M. *SHELXL-97*; 97−2 ed.; University of Goettingen: Goettingen, Germany, 1997.